# Electron-exciton interactions in the exciton-polaron problem

Dmitry K. Efimkin,[1,*] Emma K. Laird,[1] Jesper Levinsen,[1] Meera M. Parish,[1] and Allan H. MacDonald[2]
[1]*School of Physics and Astronomy and ARC Centre of Excellence in Future Low-Energy Electronics Technologies, Monash University, Victoria 3800, Australia*
[2]*The Center for Complex Quantum Systems, The University of Texas at Austin, Austin, Texas 78712-1192, USA*

(Received 24 November 2020; revised 22 January 2021; accepted 22 January 2021; published 10 February 2021)

Recently, it has been demonstrated that the absorption of moderately doped two-dimensional semiconductors can be described in terms of exciton polarons. In this scenario, attractive and repulsive polaron branches are formed due to interactions between a photoexcited exciton and a Fermi sea of excess charge carriers. These interactions have previously been treated in a phenomenological manner. Here, we present a microscopic derivation of the electron-exciton interactions which utilizes a mixture of variational and perturbative approaches. We find that the interactions feature classical charge-dipole behavior in the long-range limit, and that they are only weakly modified for moderate doping. We apply our theory to the absorption properties and show that the dependence on doping is well captured by a model with a phenomenological contact potential.

DOI: 10.1103/PhysRevB.103.075417

## I. INTRODUCTION

The fabrication of graphene has opened the door to the world of *flatland materials* [1–3]. This diverse family is still growing and prominently includes the transition-metal dichalcogenide (TMDC) monolayers $MoS_2$, $MoSe_2$, $WS_2$, and $WSe_2$. These are two-dimensional semiconductors featuring a direct band gap and extraordinarily strong Coulomb interactions, such that their optical properties are dominated by exciton physics (bound electron-hole pairs) even at room temperature. An important property of TMDC monolayers is a strong spin-valley splitting. Together with the possibility of valley selective light-matter coupling by using circularly polarized light, this opens avenues for spintronics and valleytronics [4,5]. The ability to combine TMDC monolayers in lateral and vertical heterostructures furthermore makes them strong candidates for optoelectronic applications (e.g., [6–10]) and promises a versatile platform for the exploration of exciton physics [11–13].

An additional advantage of TMDC monolayers is that their optical properties can be tuned by gating. The presence of excess charge carriers (electrons or holes) has been found [14–20] to split the exciton feature in absorption spectra [21] into two peaks [22]. The presence of the redshifted peak has conventionally been attributed to trions, i.e., charged and weakly coupled three-particle complexes formed by binding two electrons to one hole, or two holes to one electron [11–13]. Its binding energy $\epsilon_T$ is interpreted to be equal to the splitting between peaks in the limit of vanishing doping [23–28]. However, recent work [29–31] has argued that the three-particle picture for the additional peak is only relevant at very low doping and cannot explain the doping dependence of absorption (see, also, earlier works [32–39] where the trion scenario has been questioned). Instead, within the wide doping range where the excess-carrier Fermi energy $\epsilon_F \sim \epsilon_T$, the appropriate picture is one of excitons interacting with the degenerate Fermi sea of excess charge carriers. In this case, the excitons are dressed by excitations of the Fermi sea, forming attractive and repulsive exciton-polaron (XP) quasiparticles such as in the Fermi-polaron problem introduced in the context of cold atoms [40,41]. These quasiparticles represent a many-body generalization of exciton-electron (X-e) bound and unbound states.

The theory of absorption by XPs developed in Refs. [30,31] has naturally and successfully explained its observed doping dependence (it should be mentioned that there is an alternative picture that is based on dynamical screening and exciton-plasmon interactions [42–44]). However, there are still a number of experimentally relevant open questions that are within the focus of recent theoretical research [27,28,45–48]. These include the manifestations of the XP physics in photoluminescence (PL) and in nonlinear optical phenomena [49–52], as well as the crossover between few-particle and Fermi-polaron physics. For the latter problem, it has been recently argued [47] that predictions of XP- and trion-based absorption theories are almost indistinguishable in the limit of low doping. Another outstanding question concerns the importance of the microscopic details of the X-e interactions, which have been approximated by a phenomenological contact potential in previous work [29–31]. These details are also essential if excitons and excess charge carriers are spatially separated into different layers, a scenario that opens new avenues to control the flow of excitons [53,54].

In the present work, we have used a mixture of variational and perturbative techniques to derive the microscopic exciton-electron interactions. We have found that these interactions possess a weak doping dependence. Furthermore, they can be well approximated by a local potential which depends only on the X-e distance, and which features

*dmitry.efimkin@monash.edu

 

classical charge-dipole behavior at large separation. We find that this potential compares well to those recently obtained by other researchers [45,48], and that the resulting energy of the exciton-electron bound state agrees well with previous numerical results for the trion binding energy in the full three-body problem [20,55,56]. We compare our calculated doping dependence of the optical conductivity with that obtained in a model with a phenomenological contact potential and find that these agree very well. This indicates that including the finite range of exciton-electron interactions is not essential to capturing XP physics.

This paper is organized as follows: In Sec. II, we introduce our model for describing the optical properties of TMDC monolayers. We briefly review the phenomenological theory for XPs and then present our microscopic theory in Sec. III. We discuss the details of our microscopically derived X-e interactions in Sec. IV, and we also compare them to the recent results of other investigations. In Sec. V, we present a microscopic calculation of the optical conductivity and we describe its dependence on frequency and doping. Section VI contains discussions and a brief summary.

## II. MODEL

The low-energy electron and hole states in TMDC monolayers are concentrated near two equivalent valleys ($K$ and $K'$) and are separated by a direct band gap. In undoped monolayers, the absorption spectrum is dominated by excitons that can be selectively excited in one of the valleys by circularly polarized light. In the presence of excess charge carriers (we assume these to be electrons with the generalization to holes straightforward), the valleys are generically equally populated, which provides two Fermi seas (FSs) for the polaronic dressing of excitons. Importantly, electrons in one valley are distinguishable from the photoexcited electron hidden in the exciton, while electrons in the other valley are clearly not. The complicated interplay between the exchange and the polaronic physics with two FSs still represents a challenge for the microscopic theory of absorption. However, the effects of two FSs can be disentangled in the presence of strong valley splitting, which depletes electrons in one of the two valleys. Since the $K$ and $K'$ points are time-reversal partners, the splitting can be induced by exchange coupling to an insulating magnetic substrate [57] or by a magnetic field [58].

Two possible scenarios in the presence of strong splitting are sketched in Fig. 1. Figure 1(a) illustrates the case where the photoexcited electron is indistinguishable from the electrons in the Fermi sea. In this case, the polaronic dressing is limited by exchange physics and momentum-space restrictions (usually referred to as the Pauli-blocking effect) [59,60]. It is firmly established experimentally in the TMDCs [58,61–64] that this does not result in a splitting of the excitonic feature in absorption [65]. While at the theoretical level the role of exchange physics on the absorption peaks is understood only at very low doping [20], this problem is outside the scope of the present work. The dressing by a distinguishable Fermi sea is sketched in Fig. 1(b). Due to the absence of both exchange physics and the Pauli-blocking effect, this regime is more favorable for polaronic physics, and it is the scenario considered in the current work.

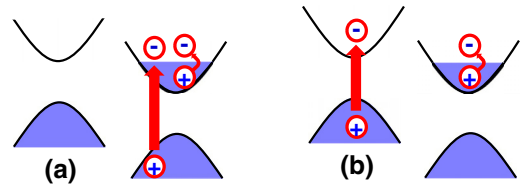


FIG. 1. Low-energy region of the TMDC band structure in the presence of strong valley imbalance. Selective coupling with circularly polarized light leads to the creation of exciton polarons dressed solely by either (a) the indistinguishable or (b) the distinguishable Fermi sea. The second band arrangement (b) is considered in the present work.

The physics of XPs for the band arrangement shown in Fig. 1(b) can be described by the Hamiltonian, $H = H_0 + H_C + H_{LM}$, which includes the kinetic energy $H_0$, Coulomb interactions $H_C$, and light-matter interactions $H_{LM}$. The first of these is given by

$$H_0 = \sum_{\mathbf{p}} \left[\epsilon^{e}_{\mathbf{p}} e^{\dagger}_{\mathbf{p}} e_{\mathbf{p}} + \epsilon^{h}_{\mathbf{p}} h^{\dagger}_{\mathbf{p}} h_{\mathbf{p}} + \epsilon^{f}_{\mathbf{p}} f^{\dagger}_{\mathbf{p}} f_{\mathbf{p}}\right]. \tag{1}$$

Here, $e^{\dagger}_{\mathbf{p}}$ and $h^{\dagger}_{\mathbf{p}}$ are the creation operators for photoexcited electrons and holes, respectively, with $f^{\dagger}_{\mathbf{p}}$ the operator for excess electrons. The band masses for electrons and holes in monolayer TMDCs can be well approximated as equal to each other. Thus, we take the dispersions to be $\epsilon^{e(h)}_{\mathbf{p}} = \epsilon_g/2 + p^2/2m$ (with $p \equiv |\mathbf{p}|$) and $\epsilon^{f}_{\mathbf{p}} = p^2/2m - \epsilon_F$, where $\epsilon_g$ is the gap in the spectrum and $\epsilon_F$ is the Fermi energy of excess charge carriers. Note that in this work, we employ Gaussian units ($4\pi\varepsilon_0 = 1$) and we additionally set the system area to unity.

The Coulombic interactions can be modeled by

$$H_C = \sum_{\mathbf{p}\bar{\mathbf{p}}\mathbf{q}} U_{\mathbf{q}} [e^{\dagger}_{\mathbf{p}+\mathbf{q}} f^{\dagger}_{\bar{\mathbf{p}}-\mathbf{q}} f_{\bar{\mathbf{p}}} e_{\mathbf{p}} - h^{\dagger}_{\mathbf{p}+\mathbf{q}} f^{\dagger}_{\bar{\mathbf{p}}-\mathbf{q}} f_{\bar{\mathbf{p}}} h_{\mathbf{p}} - e^{\dagger}_{\mathbf{p}+\mathbf{q}} h^{\dagger}_{\bar{\mathbf{p}}-\mathbf{q}} h_{\bar{\mathbf{p}}} e_{\mathbf{p}}], \tag{2}$$

where we neglect intraspecies interactions since these do not significantly affect the absorption [66]. Here, $U_{\mathbf{q}}$ is the Coulomb interaction potential and our developed microscopic theory for exciton polarons does not rely on its explicit form. For numerical calculations, we employ the two-dimensional (2D) Coulomb potential, $U_{\mathbf{q}} = 2\pi e^2/\kappa q$, with $\kappa$ the effective dielectric constant of the surrounding media. However, we argue that our results are much more general and can be extended to other screening models, including the Keldysh potential [67–69]. The Keldysh potential properly handles dielectric screening and is argued to quite accurately capture the spectrum of excitonic states in TMDC monolayers [17,70].

Within the dipole approximation, light-matter interactions can be described by using a position-independent vector potential $\mathbf{A}$ as follows:

$$H_{LM} = -\frac{ev}{c} \sum_{\mathbf{p}} \mathbf{A} \cdot [\mathbf{e}\, e^{\dagger}_{\mathbf{p}} h^{\dagger}_{-\mathbf{p}} e^{-i\omega t} + \text{H.c.}]. \tag{3}$$

The light frequency satisfies $\omega \sim \epsilon_g \gg \epsilon_F$, which allows us to neglect intraband electronic transitions. Above, $v = \sqrt{\epsilon_g/m}$ is the interband matrix element for the velocity operator, and

$\mathbf{e} = (\mathbf{e}_x \pm i\mathbf{e}_y)/\sqrt{2}$ determines the valley selection by circularly polarized light. We elaborate on the absorption theory in Sec. V, while the two subsequent sections are devoted to our microscopic theory for XPs.

## III. EXCITON-POLARON THEORY

### A. Exciton problem

Within our model, the exciton can be described by the creation operator

$$X^\dagger_{\mathbf{p}_X} = \sum_{\mathbf{p}} C_{\mathbf{p}} e^\dagger_{\mathbf{p}+\mathbf{p}_X/2} h^\dagger_{-\mathbf{p}+\mathbf{p}_X/2}. \tag{4}$$

Here, $C_{\mathbf{p}}$ is the wave function for the relative motion of the electron and hole. Note that it does not depend on the exciton's center-of-mass momentum, $\mathbf{p}_X$. This is because there is a separation of relative and center-of-mass dynamics in the two-body problem with a conventional quadratic spectrum. The wave function $C_{\mathbf{p}}$ satisfies the following eigenvalue equation:

$$(\epsilon^e_{\mathbf{p}} + \epsilon^h_{-\mathbf{p}})C_{\mathbf{p}} - \sum_{\mathbf{p}'} U_{\mathbf{p}-\mathbf{p}'} C_{\mathbf{p}'} = E^X C_{\mathbf{p}}, \tag{5}$$

with total energy $E^X$. The resulting spectrum includes both discrete excitonic states and continuous unbound electron-hole pairs, and we label these states by a collective index, $\nu$. The bound excitonic states are labeled by principal $n$ and orbital $l$ quantum numbers, $|\nu\rangle = |n, l\rangle$ (with $|0, 0\rangle$ corresponding to the ground-state exciton).

### B. Phenomenological approach

For completeness, here we briefly review the theory of exciton polarons with phenomenological contact exciton-electron interactions [29–31]. Its cornerstone is the hierarchy of binding energies for trions ($\epsilon_T$) and excitons ($\epsilon_X$), i.e., $\epsilon_T \ll \epsilon_X$. This ensures that in the wide density range where $\epsilon_T \sim \epsilon_F$, the formation of an exciton by a photoexcited electron and hole is only weakly disturbed by excess charge carriers. In this limit, it is therefore reasonable to consider the exciton as a structureless quasiparticle where the center-of-mass momentum is the only relevant degree of freedom.

The exciton's interaction with the Fermi sea dresses it into an exciton polaron. The corresponding Fermi-polaron problem (involving a Fermi sea as a quantum environment) has recently been realized in 2D cold-atom experiments [71–73], and a remarkable understanding of its rich behavior has been achieved [40,41]. The creation operator for an optically active XP with zero momentum can be well approximated by the Chevy ansatz [74] as follows:

$$P^\dagger_{\mathbf{0}} = \phi X^\dagger_{\mathbf{0}} + \sum_{\mathbf{kk}'} \chi_{\mathbf{kk}'} X^\dagger_{\mathbf{k}'-\mathbf{k}} f^\dagger_{\mathbf{k}} f_{\mathbf{k}'}. \tag{6}$$

Above, $\phi$ is the weight of the exciton, while $\chi_{\mathbf{kk}'}$ weights the contribution of a single electron-hole pair excitation of the FS with momenta $k > k_F$ and $k' < k_F$. The possibility to excite multiple electron-hole pairs has been proven to be negligibly small [75]. The photoexcited electron and hole interact both with the electron outside the FS and with the hole inside the FS. However, momentum-space limitations mean that the latter is inefficient for $\epsilon_F \ll \epsilon_X$ and can therefore be omitted. If we introduce the exciton-electron interactions in a phenomenological manner as $V_{\mathbf{q}}$, then the variational equations for the state (6) are given by

$$\left(\Delta E^{XP} - \sum_{\mathbf{k}'} V_{\mathbf{0}}\right)\phi = \sum_{\mathbf{kk}'} V_{\mathbf{k}-\mathbf{k}'} \chi_{\mathbf{kk}'}, \tag{7a}$$

$$(\Delta E^{XP} - \epsilon^{FS}_{\mathbf{kk}'})\chi_{\mathbf{kk}'} = V_{\mathbf{k}'-\mathbf{k}}\phi + \sum_{\bar{\mathbf{k}}} V_{\bar{\mathbf{k}}-\mathbf{k}} \chi_{\bar{\mathbf{k}}\mathbf{k}'}. \tag{7b}$$

Here, $\epsilon^{FS}_{\mathbf{kk}'} = \epsilon^X_{\mathbf{k}'-\mathbf{k}} + \epsilon^f_{\mathbf{k}} - \epsilon^f_{\mathbf{k}'}$ is the sum of kinetic energies for the exciton's center of mass and an electron-hole excitation of the Fermi sea. The quantity $\Delta E^{XP} = E^{XP} - E^X$ is the energy of the exciton-polaron state $E^{XP}$ defined with respect to the exciton energy $E^X$. Due to the Pauli-blocking effect of electrons in the FS, the momentum in the last sum of Eq. (7) is restricted to $\bar{k} > k_F$.

If $V_{\mathbf{q}}$ is approximated by a contact potential with a momentum-independent Fourier transform, then the system of equations becomes algebraic [76] and analytically tractable [77]. Its solution can be elegantly parameterized by the binding energy $\epsilon_T$ for the two-particle X-e state, which is a simplified model for the trion. The energy $\epsilon_T$ determines the splitting between attractive and repulsive XP branches in the limit of vanishing doping, and therefore can be easily adjusted to fit experiments. The frequency and doping dependence of absorption within this model has been extensively discussed in our previous work [30] and has been argued to well describe the experimental data.

### C. Microscopic theory

To derive the microscopic theory for XPs, we avoid using excitons as an intermediate step of the theory. Instead, we write the creation operator for an XP with zero momentum as follows:

$$P^\dagger_{\mathbf{0}} = \sum_{\mathbf{p}} \phi_{\mathbf{p}} e^\dagger_{\mathbf{p}} h^\dagger_{-\mathbf{p}} + \sum_{\mathbf{pkk}'} \chi_{\mathbf{pkk}'} e^\dagger_{\mathbf{p}_+} h^\dagger_{-\mathbf{p}_-} f^\dagger_{\mathbf{k}} f_{\mathbf{k}'}. \tag{8}$$

Here, $\mathbf{p}_\pm = \mathbf{p} \pm (\mathbf{k}' - \mathbf{k})/2$ and $\mathbf{k}' - \mathbf{k}$ is the center-of-mass momentum for the photoexcited electron and hole. In addition, $\phi_{\mathbf{p}}$ is the wave function for the relative motion of the electron-hole pair, while $\chi_{\mathbf{pkk}'}$ weights its correlations with a single particle-hole excitation of the Fermi sea. By neglecting interactions between the excitonic electron or hole and the Fermi-sea hole, since these are inefficient due to momentum-space limitations, we obtain the variational expressions shown below,

$$(\epsilon^e_{\mathbf{p}} + \epsilon^h_{-\mathbf{p}})\phi_{\mathbf{p}} - \sum_{\bar{\mathbf{p}}} U_{\mathbf{p}\bar{\mathbf{p}}}\phi_{\bar{\mathbf{p}}} + \sum_{\mathbf{kk}'} U_{\mathbf{k}-\mathbf{k}'}\left(\chi_{\mathbf{p}-\frac{\mathbf{k}-\mathbf{k}'}{2},\mathbf{kk}'} - \chi_{\mathbf{p}+\frac{\mathbf{k}-\mathbf{k}'}{2},\mathbf{kk}'}\right) = E^{XP}\phi_{\mathbf{p}} \tag{9}$$

and

$$\begin{aligned}(\epsilon^e_{\mathbf{p}} + \epsilon^h_{-\mathbf{p}} + \epsilon^{FS}_{\mathbf{kk}'})\chi_{\mathbf{pkk}'} &- \sum_{\bar{\mathbf{p}}} U_{\mathbf{p}-\bar{\mathbf{p}}}\chi_{\bar{\mathbf{p}}\mathbf{kk}'} \\ &+ \sum_{\bar{\mathbf{k}}} U_{\bar{\mathbf{k}}-\mathbf{k}}\left(\chi_{\mathbf{p}-\frac{\bar{\mathbf{k}}-\mathbf{k}}{2},\bar{\mathbf{k}}\mathbf{k}'} - \chi_{\mathbf{p}+\frac{\bar{\mathbf{k}}-\mathbf{k}}{2},\bar{\mathbf{k}}\mathbf{k}'}\right) \\ &+ U_{\mathbf{k}'-\mathbf{k}}\left(\phi_{\mathbf{p}-\frac{\mathbf{k}'-\mathbf{k}}{2}} - \phi_{\mathbf{p}+\frac{\mathbf{k}'-\mathbf{k}}{2}}\right) = E^{XP}\chi_{\mathbf{pkk}'}.\end{aligned} \tag{10}$$

Due to the presence of the Fermi sea, the momenta are restricted to $k,\ \bar{k} > k_{\rm F}$, and $k' < k_{\rm F}$ above and in what follows. For the considered doping range $\epsilon_{\rm F} \ll \epsilon_{\rm X}$, the relative motion of the electron and hole within the exciton is only weakly disturbed by excess electrons. This motivates the decomposition of both wave functions, $\phi_{\mathbf{p}}$ and $\chi_{\mathbf{pkk'}}$, into the excitonic (and continuum) states discussed in Sec. III A,

$$\phi_{\mathbf{p}} = \sum_{\nu} C^{\nu}_{\mathbf{p}} \phi_{\nu}, \quad \chi_{\mathbf{pkk'}} = \sum_{\nu} C^{\nu}_{\mathbf{p}} \chi_{\nu\mathbf{kk'}}. \tag{11}$$

The variational equations can then be rewritten as

$$\Delta E^{\rm XP}_{\nu} \phi_{\nu} = \sum_{\bar{\nu}\mathbf{kk'}} \Lambda^{\nu\bar{\nu}}_{\mathbf{k}-\mathbf{k'}} \chi_{\bar{\nu}\mathbf{kk'}}, \tag{12a}$$

$$\left(\Delta E^{\rm XP}_{\nu} - \epsilon^{\rm FS}_{\mathbf{kk'}}\right)\chi_{\nu\mathbf{kk'}} = \sum_{\bar{\nu}} \Lambda^{\nu\bar{\nu}}_{\mathbf{k'}-\mathbf{k}} \phi_{\bar{\nu}} + \sum_{\bar{\nu}\bar{\mathbf{k}}} \Lambda^{\nu\bar{\nu}}_{\bar{\mathbf{k}}-\mathbf{k}} \chi_{\bar{\nu}\bar{\mathbf{k}}\mathbf{k'}}, \tag{12b}$$

where we denote $\Delta E^{\rm XP}_{\nu} = E^{\rm XP} - E^{\rm X}_{\nu}$. The excitonic levels are coupled by the matrix element $\Lambda^{\nu\bar{\nu}}_{\mathbf{q}}$, which represents the amplitude of X-e scattering between states $|i_\nu\rangle = X^{\dagger}_{\nu\mathbf{p}_{\rm X}} f^{\dagger}_{\mathbf{p}_{\rm e}}|{\rm g}\rangle$ and $|f_\nu\rangle = X^{\dagger}_{\nu\mathbf{p}_{\rm X}+\mathbf{q}} f^{\dagger}_{\mathbf{p}_{\rm e}-\mathbf{q}}|{\rm g}\rangle$ (where $|{\rm g}\rangle$ is the undisturbed Fermi sea). The scattering amplitude, with transferred momentum $\mathbf{q}$, in the Born approximation is given by

$$\Lambda^{\nu\bar{\nu}}_{\mathbf{q}} = \langle f_\nu|(H_{\text{e-f}} + H_{\text{h-f}})|i_{\bar{\nu}}\rangle. \tag{13}$$

Here, $H_{\text{e-f}}$ and $H_{\text{h-f}}$ represent, respectively, the interaction between a Fermi-sea electron and the electron or hole that constitutes the exciton. They correspond to the first two terms in Eq. (2). The explicit expression for the scattering matrix element is

$$\Lambda^{\nu\bar{\nu}}_{\mathbf{q}} = U_{\mathbf{q}} \sum_{\mathbf{p}} \left(C^{\nu}_{\mathbf{p}}\right)^{*} \left(C^{\bar{\nu}}_{\mathbf{p}-\mathbf{q}/2} - C^{\bar{\nu}}_{\mathbf{p}+\mathbf{q}/2}\right). \tag{14}$$

We can further comprehend the nature of $\Lambda^{\nu\bar{\nu}}_{\mathbf{q}}$ by now considering its behavior at small momentum transfer, $qa_{\rm X} \ll 1$, with $a_{\rm X}$ the exciton size. By introducing $C^{\nu}_{\mathbf{r}}$ as the Fourier transform of $C^{\nu}_{\mathbf{p}}$ in Eq. (14), we find that

$$\Lambda^{\nu\bar{\nu}}_{\mathbf{q}} = U_{\mathbf{q}} \int d\mathbf{r} \left(C^{\nu}_{\mathbf{r}}\right)^{*} C^{\bar{\nu}}_{\mathbf{r}}\, 2i \sin\left(\frac{\mathbf{q}\cdot\mathbf{r}}{2}\right) \tag{15a}$$

$$\simeq i U_{\mathbf{q}} \mathbf{q}\cdot\mathbf{d}_{\nu\bar{\nu}}, \quad qa_X \ll 1, \tag{15b}$$

where $e\mathbf{d}_{\nu\bar{\nu}} = \langle\nu|e\mathbf{r}|\bar{\nu}\rangle$ is the matrix element of the dipole moment. This explicitly reflects the charge-dipole nature of exciton-electron interactions. Since $|\nu\rangle$ is a parity eigenstate, $\Lambda^{\nu\bar{\nu}}_{\mathbf{q}}$ follows the selection rules for optical dipole transitions between the excitonic states. Therefore, $\Lambda^{\nu\bar{\nu}}_{\mathbf{q}}$ is nonzero only between states of opposite parities, which implies that $l - \bar{l} = \pm 1, \pm 3, \ldots$. Consequently, the diagonal matrix elements vanish, $\Lambda^{\nu\nu}_{\mathbf{q}} = 0$, and we emphasize that only those elements coupling distinct excitonic (and continuum) states are nonzero.

To proceed, we restrict our attention to the effect of the excess electrons on only the ground excitonic state. The corresponding exciton-polaron state predominantly consists of $\phi \equiv \phi_\nu$ and $\chi_{\mathbf{kk'}} \equiv \chi_{\nu\mathbf{kk'}}$, with $|\nu\rangle = |0,0\rangle$. Provided that $\epsilon_{\rm F}, \epsilon_{\rm T} \ll \epsilon_{\rm X}$, the contribution of all excited states is small. Interactions between them are of second order in $\epsilon_{\rm T}/\epsilon_{\rm X}$ and can therefore be neglected. If we treat the coupling of excited states to (only) the ground state $|0,0\rangle$ perturbatively, then Eq. (12) simplifies to

$$\left(\Delta E^{\rm XP}_0 - \sum_{\mathbf{k'}} V_{\mathbf{k'k'k'}}\right)\phi = \sum_{\mathbf{kk'}} V_{\mathbf{kk'k'}} \chi_{\mathbf{kk'}}, \tag{16a}$$

$$\left(\Delta E^{\rm XP}_0 - \epsilon^{\rm FS}_{\mathbf{kk'}}\right)\chi_{\mathbf{kk'}} = V_{\mathbf{k'kk'}}\phi + \sum_{\bar{\mathbf{k}}} V_{\bar{\mathbf{k}}\mathbf{kk'}} \chi_{\bar{\mathbf{k}}\mathbf{k'}}. \tag{16b}$$

For a detailed derivation, we refer the reader to Appendix A.

This set of equations remarkably coincides with the variational expressions (7) obtained previously within the phenomenological approach. However, the microscopically derived interactions,

$$V_{\mathbf{k}_1\mathbf{k}_2\mathbf{k'}} = \sum_{\nu\mathbf{k}} \frac{\Lambda^{0\nu}_{\mathbf{k}-\mathbf{k}_2} \Lambda^{\nu 0}_{\mathbf{k}_1-\mathbf{k}}}{E^{\rm X}_0 - E^{\rm X}_{\nu} - \epsilon^{\rm FS}_{\mathbf{kk'}}}, \tag{17}$$

are intrinsically nonlocal and depend explicitly on the momentum of the electron before ($\mathbf{k}_2$) and after ($\mathbf{k}_1$) scattering with the exciton, as well as on the momentum of the redundant Fermi hole ($\mathbf{k}'$) which does not participate directly in the scattering process. Note that we have taken $E^{\rm XP} \simeq E^{\rm X}_0$ in the denominator of Eq. (17). This approximation makes Eq. (16) tractable and is reasonable because the total energy is only shifted away from the exciton energy by a small amount (of the order of $\epsilon_{\rm F}, \epsilon_{\rm T} \ll \epsilon_{\rm X}$).

The cornerstone relation of the exciton-polaron theory is the hierarchy of scales, $\epsilon_{\rm F} \sim \epsilon_{\rm T} \ll \epsilon_{\rm X}$, ensuring that the theory is applicable in a wide range of density of excess charge carriers. At very low doping, $\epsilon_{\rm F} \ll \epsilon_{\rm T}$, three-particle correlations not captured by the theory may be expected to be important. However, predictions of trion and exciton-polaron scenarios have been recently found to be almost indistinguishable in this regime [47], thus suggesting that the theory is also applicable at low doping.

Note that our arguments thus far do not specify the interaction between electrons and holes, $U_{\mathbf{q}}$, which relies on details of the screening (dielectric or metallic) due to the surrounding media. For this reason, our developed theory is applicable to monolayer semiconductors as well as to conventional semiconductor quantum wells (QWs). In the following, for simplicity, we have chosen to use the 2D Coulomb potential, $U_{\mathbf{q}} = 2\pi e^2/\kappa q$, where $\kappa$ is the effective dielectric constant of the surrounding environment. While this potential properly captures only the excited excitonic states including the continuous part of the spectrum, analytic expressions for the wave functions $C^{\nu}_{\mathbf{p}}$ are known, which considerably simplifies the numerics. These wave functions are provided in Appendix B. (Note that the entire spectrum is reasonably well described by the Keldysh potential [67–69], which properly incorporates the dielectric screening in layered systems [17,70].) In the discussion in Sec. VI, we argue that our results are very general and therefore extendable to other potentials.

## IV. EXCITON-ELECTRON INTERACTIONS

The excitonic spectrum with 2D Coulomb interactions, $U_{\mathbf{q}} = 2\pi e^2/\kappa q$, admits an analytical solution which has been extensively discussed in Refs. [78–80] and is summarized

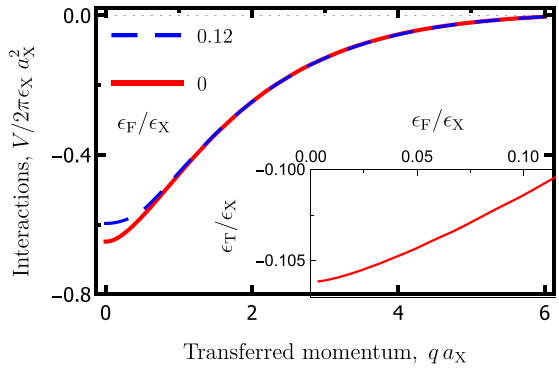


FIG. 2. Fourier transform of the X-e interactions at doping levels $\epsilon_F = 0$ (solid red line) and $\epsilon_F = 0.12\,\epsilon_X$ (dashed blue line). The inset shows the weak doping dependence for the binding energy $\epsilon_T$ of the two-particle X-e bound state.

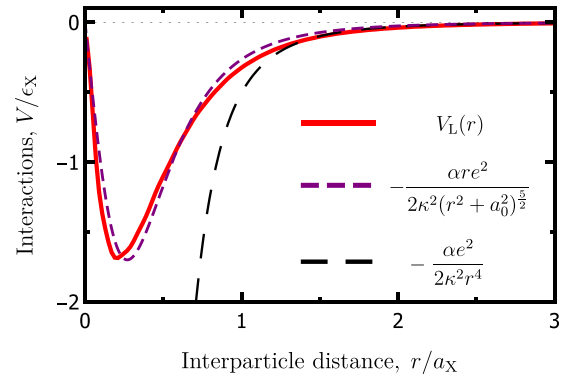


FIG. 3. Spatial profile of the local X-e interaction $V_L(\mathbf{r})$ (solid red line), its approximation by a modified charge-dipole potential $V_A(\mathbf{r})$ (dashed purple line), and the asymptotic behavior at large interparticle distance (dashed black line).

in Appendix B. The spectrum of discrete states, $E_\nu^X = -\epsilon_X/(2n+1)^2$ where $|\nu\rangle = |n, l\rangle$, possesses accidental degeneracy, which is typical for Coulomb problems [80]. Here, $\epsilon_X = \hbar^2/ma_X^2 = me^4/\hbar^2\kappa^2$ is the binding energy of the excitonic ground state $|\nu\rangle = |0, 0\rangle$, and $a_X = \hbar^2\kappa/me^2$ is the average electron-hole separation in that state. The continuous spectrum of unbound electron-hole pairs, $E_\nu^X = q^2\epsilon_X$, can be labeled $|\nu\rangle = |q, l\rangle$ by a dimensionless absolute momentum $q$ and an orbital quantum number $l$. For numerical calculations of the effective X-e interactions, we have taken into account excitonic states with $n = 1, \ldots, 10$ and $|l| = 1,\ 3,\ 5$ as well as the whole continuous spectrum with $|l| = 1,\ 3$. We have checked that the contribution of truncated states is negligibly small.

The derived X-e interaction (17) is doping dependent and nonlocal in nature. However, it is instructive to introduce its simplified doping-dependent *local* counterpart,

$$V_L(\mathbf{q}) = V_{\mathbf{q},\mathbf{0},\mathbf{0}} = V_{\mathbf{0},\mathbf{q},\mathbf{0}}. \tag{18}$$

This local potential is solely determined by the transferred momentum $\mathbf{q}$, which implies that the corresponding real-space potential $V_L(\mathbf{r})$ only depends on the relative distance between the exciton and electron.

Due to the hierarchy of energy scales $\epsilon_F,\ \epsilon_T \ll \epsilon_X$, the spatial scale over which the polaronic correlations occur can be estimated by $a_T \approx a_X\sqrt{\epsilon_X/\epsilon_T} \approx 3a_X$. This implies that the details of the real-space potential profile, corresponding to Eq. (17), are most important at $r \gtrsim a_X$. A careful numerical comparison of the nonlocal (17) and local (18) potentials is presented in Appendix D, and there we show how the latter very well approximates the interactions for $qa_X \ll 1$. Evidently, the nonlocal nature of X-e interactions is unimportant and, at $r \gtrsim a_X$, they are well captured by Eq. (18), which we use below.

The resulting local interactions $V_L(\mathbf{q})$ at zero doping and at doping $\epsilon_F = 0.12\,\epsilon_X$ are presented in Fig. 2. The doping dependence of the interaction is weak and its dependence on momentum at $qa_X \ll 1$ is smooth. This is a signature of the short-range nature of the interactions and it presents an additional justification for the contact phenomenological potential that has been used previously [29–31].

In the limit of vanishing doping, the polaronic physics reduces to the two-particle X-e problem. Their bound state represents a simplified model for the trion and its binding energy is shown in the inset of Fig. 2. It has a very weak doping dependence and is equal to $\epsilon_T^\star = 0.106\,\epsilon_X$ at $\epsilon_F = 0$. This energy is quite close to the numerical solution for the three-particle trion problem, $\epsilon_T = 0.118\,\epsilon_X$, with 2D Coulomb interactions [20,55,56]. This suggests that the low-doping regime $\epsilon_F \ll \epsilon_T$ is also properly captured by the polaronic theory, in agreement with the conclusions of Ref. [47] where a detailed comparison of the predictions of trion and XP theories is presented. The origin of the small discrepancy with the numerical solution for $\epsilon_T$ is the perturbative treatment of the excited exciton states—not the local approximation of interactions given by Eq. (18).

The spatial dependence of the interactions at $\epsilon_F = 0$ is presented in Fig. 3, and it can be accurately approximated by the following expression:

$$V_A(\mathbf{r}) = \frac{\alpha e^2 r}{2\kappa^2\left(r^2 + a_0^2\right)^{\frac{5}{2}}}. \tag{19}$$

Here, $a_0 \approx 0.54\,a_X$, and $\alpha$ is the polarizability of the ground state $|0, 0\rangle$ which, within second-order perturbation theory, is calculated to be

$$\alpha = \sum_\nu \frac{|\mathbf{d}_{0\nu}|^2}{E_0^X - E_\nu^X}. \tag{20}$$

As before, $\mathbf{d}_{0\nu}$ is the matrix element for the dipole moment between the excitonic ground state and an excited state $|\nu\rangle$. It is clearly seen in Fig. 3 that the potential perfectly follows the classical charge-dipole interaction, $-\alpha e^2/2\kappa^2 r^4$ at $r \gtrsim a_X$, which is the relevant region for polaronic physics. For this reason, we refer to the microscopically derived interaction (17) as a charge-dipole potential.

Numerically, we find that the contributions of discrete excitonic states ($\alpha_D \approx 2\alpha/3$) and unbound electron-hole pairs ($\alpha_C \approx \alpha/3$) to the polarizability of the exciton are comparable with each other. Thus, the latter is important and cannot be truncated within the microscopic XP theory. It should also be mentioned that the low-energy continuum states cannot be

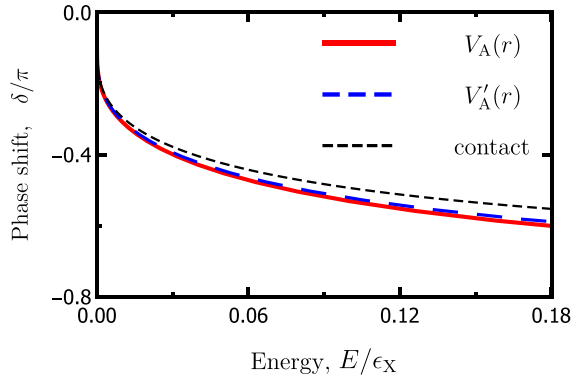


FIG. 4. Energy dependence of the X-e scattering phase shift $\delta(E)$ with the interactions approximated by $V_A(\mathbf{r})$ (solid red line) and $V'_A(\mathbf{r})$ (long-dashed blue line). The result for the contact potential which reproduces the X-e binding energy $\epsilon_T^\star$ is also shown for comparison (short-dashed black line). For all considered interactions, the phase shift approaches $\delta = -\pi$ for $E \gg \epsilon_X$.

approximated by plane waves due to the presence of Gamow-Sommerfeld enhancement [81].

The interactions between excitons and electrons have also been recently addressed through other approaches. In particular, a comprehensive analysis [48] of the energy-dependent phase shifts $\delta(E)$ for X-e scattering has demonstrated that their low-energy behavior is well captured by the following modified charge-dipole interaction:

$$V'_A(\mathbf{r}) = \begin{cases} -\frac{\alpha}{2}\left(\frac{\partial U}{\partial r}\right)^2, & r > a_*, \\ V_*, & r < a_*, \end{cases} \tag{21}$$

which, importantly, features the same functional form of the long-range interactions. Here, the potential $V_*$ and length $a_*$ (which is comparable to the exciton radius $a_X$) are parameters used for the fitting of $\delta(E)$ calculated numerically within the three-particle problem. Within the spatial range relevant for the polaronic correlations, $r \gtrsim a_T \sim 3a_X$, the potential $V'_A$ follows the classical charge-dipole behavior in the same manner as $V_A(\mathbf{r})$ in Eq. (19). However, they have different short-range behavior at $r \lesssim a_X$. In Ref. [48], the interactions $U(\mathbf{r})$ were approximated by the Keldysh potential, which complicates a direct comparison between $V_A$ and $V'_A$; however, we may still compare the general behavior of the resulting X-e scattering. To investigate the importance of short-range details for the X-e potentials, we therefore instead use 2D Coulomb interactions, $U(\mathbf{r}) = e^2/\kappa r$, and we choose the potential $V'_A$ to be continuous, which implies that $V_* = -\alpha e^2/2\kappa^2 a_*^4$. We then adjust the length $a_* = 0.866\, a_X$ such that the potential $V'_A$ reproduces the binding energy of the exciton-electron bound state $\epsilon_T^\star$ in this simplified model for the formation of a trion. The resulting energy dependence of the scattering phase shift $\delta(E)$ is presented in Fig. 4, where we see that the results for $V_A$ and $V'_A$ are almost indistinguishable, demonstrating that the short-range details of the potentials are not important. We can further illustrate this point by comparing with the universal form of the phase shift calculated from a contact exciton-electron potential that reproduces the same binding energy, $\cot\delta(E) = \frac{1}{\pi}\ln(E/\epsilon_T^\star)$. We see that the phase shifts obtained within the potentials $V_A$ and $V'_A$ can be reasonably described by contact interactions, which does not agree with the conclusions of Ref. [48]. Our calculations, therefore, suggest that the screening of electronic interactions is essential to resolve this discrepancy.

Previous work has argued that the X-e interactions can be extracted directly from the matrix element of their scattering, $V_S(\mathbf{q}) = \Lambda_{\mathbf{q}}^{00}$ [45,82,83]. Its magnitude and sign were shown to be very sensitive to the ratio between the electron $m_e$ and hole $m_h$ masses. In particular, for the balanced case considered here where $m_e = m_h$, $V_S(\mathbf{q})$ is zero due to parity arguments and it is therefore insensitive to the details of the interaction potential $U_\mathbf{q}$ between the electrons and holes [84]. Therefore, our theory represents the minimal level of perturbation theory necessary to describe the experimentally relevant case of TMDC monolayers.

The matrix element $V_S(\mathbf{q})$ can be nonzero in the presence of the exchange channel that appears if the electron within the exciton and those of the Fermi sea are indistinguishable. This is relevant in the case of intravalley exciton-electron correlations in TMDC monolayers and spin-triplet ones in semiconductor QWs; however, this effect is outside the scope of the present work.

We conclude that the interactions between an exciton and an electron of the Fermi sea, given by Eq. (17), are very well approximated by the local and doping-independent interactions in Eq. (19) that are derived from the two-particle exciton-electron problem. We use the latter in our numerical calculations of absorption by XPs.

## V. ABSORPTION OF EXCITON POLARONS

### A. Derivation of optical conductivity

The absorption of a semiconductor is determined by the real part of its optical conductivity $\sigma(\omega)$. Within linear-response (Kubo) theory, this can be approximated by [85]

$$\sigma(\omega) = \frac{\pi}{2\epsilon_g}\sum_\mu |\langle g|\mathbf{J}|\mu\rangle|^2 \delta\left(\hbar\omega - E_\mu^{XP}\right). \tag{22}$$

Above, $\mathbf{J} = ev\mathbf{e}\sum_\mathbf{p} e_\mathbf{p} h_{-\mathbf{p}} + \text{H.c.}$ is the electric current operator restricted to intraband transitions. Its matrix element is calculated between the ground state, $|g\rangle = \Pi_{k'<k_F} f^\dagger_{\mathbf{k}'}|\text{vac}\rangle$, and the polaronic state with zero momentum, $|\mu\rangle = P^\dagger_{\mu\mathbf{0}}|g\rangle$. The index $\mu$ labels an eigenstate of the polaronic equations (16) with energy $E_\mu^{XP}$. The corresponding matrix element is given by

$$\langle g|\mathbf{J}|\mu\rangle = ev\mathbf{e}\sum_\mathbf{p}\phi_{\mu\mathbf{p}} = ev\mathbf{e}\sum_\nu C^\nu_{\mathbf{r}=0}\phi_{\mu\nu}. \tag{23}$$

Here, we have used the decomposition $\phi_{\mu\mathbf{p}} = \sum_\nu C^\nu_\mathbf{p}\phi_{\mu\nu}$ in terms of the excitonic states $C^\nu_\mathbf{p}$, as written in (11). The contribution of excited states is small at $\epsilon_F \ll \epsilon_X$ and we only keep the contribution of the ground state, $\phi_\mu \equiv \phi_{\mu 0}$. If we assume that the light is circularly polarized and note that $C^0_{\mathbf{r}=0} = \sqrt{2/\pi a_X^2}$, then the optical conductivity (22) simplifies as follows:

$$\sigma(\omega) = \sigma_0\epsilon_X\sum_\mu 2\pi|\phi_\mu|^2\delta\left(\omega - E_\mu^{XP}\right) = \sigma_0\epsilon_X A_X(\omega). \tag{24}$$

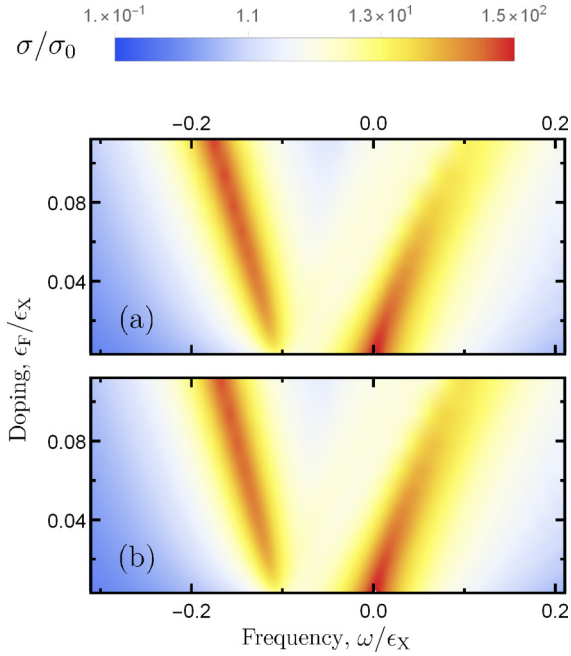


FIG. 5. Optical conductivity $\sigma(\omega)/\sigma_0$, where $\sigma_0 = e^2/h$ is the quantum unit of conductance. Interactions between an exciton and a Fermi sea of excess charge carriers are approximated by either (a) a charge-dipole or (b) a contact potential, which causes the excitonic absorption feature to split into attractive and repulsive exciton-polaron branches.

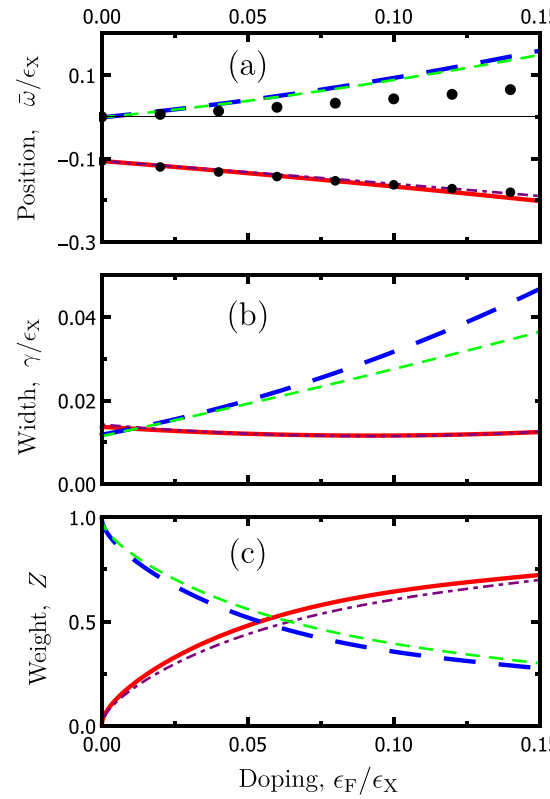


FIG. 6. Doping dependence of the (a) peak position, (b) peak width, and (c) the associated spectral weight. The solid red and long-dashed blue lines correspond, respectively, to the attractive and repulsive XP branches calculated by using charge-dipole interactions. The dot-dashed purple and short-dashed green lines likewise correspond to those calculated for contact interactions. Black dots in (a) correspond to the model with infinite exciton mass and are evaluated with Eqs. (25).

Above, $\sigma_0 = e^2/2\pi\hbar$ is the conductivity quantum and we have introduced the spectral function for excitons dressed into XPs, $A_X(\omega)$. The latter naturally appears in the diagrammatic theory for XPs [29–31]. The frequency dependence of the absorption is completely determined from the spectral function, and we have numerically calculated this by using the variational equations (16) for XPs with local doping-dependent interactions (18).

### B. Doping dependence of optical conductivity

We now proceed to compare the predictions of our parameter-free microscopic theory for XPs with those of the phenomenological approach. To this end, we need to adjust $\epsilon_T$ in the latter, since this is the only free parameter. We have chosen to use $\epsilon_T^\star$, which represents the binding energy for the two-body X-e state. The numerical calculations require a broadening [86], and thus we replace $\delta(\omega) \to (\gamma_X/\pi)/(\omega^2 + \gamma_X^2)$, where we take $\gamma_X = 0.1\,\epsilon_T^\star$. Physically, such a broadening can originate from the radiative decay of excitons or from their scattering due to disorder or phonons; all of these effects are inevitably present in real materials.

The doping and frequency dependence of the optical conductivity $\sigma(\omega)$ are presented in Fig. 5, both for our charge-dipole interactions and for the case of contact interactions [30,86]. The dressing of excitons by the Fermi sea of excess charge carriers splits them into attractive (redshifted peak) and repulsive (blueshifted) XPs. Even at a quantitative level, the predictions between contact and charge-dipole interactions agree very well, and any difference becomes apparent only at a moderate doping $\epsilon_F \sim \epsilon_T$. In the following, we characterize these attractive (A) and repulsive (R) branches by their position $\bar{\omega}_{A(R)}$, width $\gamma_{A(R)}$, and spectral weight $Z_{A(R)}$ (also commonly referred to as the oscillator strength).

The doping dependence of the peak positions $\bar{\omega}_{A(R)}$ is presented in Fig. 6(a). It is important to separate the effect of excess charge carriers on the splitting between XPs ($\Delta\bar{\omega} = \bar{\omega}_R - \bar{\omega}_A$) and their synchronous shift. The latter can also be induced by other factors (e.g., band-gap renormalization and interactions with phonons) that are material dependent and are not easy to separate and distinguish. By contrast, the splitting originates solely from the polaronic dressing and is presented in Fig. 7. The difference between the predictions of the two models becomes apparent only at $\epsilon_F \approx \epsilon_T$, but is still much smaller than $\Delta\bar{\omega}$. Importantly, within both models, the splitting increases linearly with $\epsilon_F$ as $\Delta\bar{\omega} = \epsilon_T + 3\epsilon_F/2$, which can be considered as a hallmark of Fermi polaron physics and agrees with experimental observations [14,19]. The factor $3/2$ is given by the ratio between the electron mass $m$ and the reduced exciton-electron mass $2m/3$.

It is instructive to compare these results with the predictions of the exciton-polaron model, where the exciton is taken to be infinitely heavy. This scenario is known to be exactly solvable and, according to Fumi's theorem, the positions of the peaks are related to the energy-dependent phase shifts

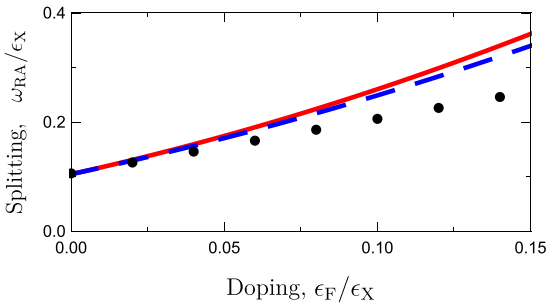


FIG. 7. Doping dependence of the splitting between the attractive and repulsive XP branches for both charge-dipole (solid red line) and contact (dashed blue line) interactions. It is well captured by relation $\Delta\bar{\omega} = \epsilon_T + 3\epsilon_F/2$. Black dots in (a) correspond to the model with infinite exciton mass that predicts $\Delta\bar{\omega} = \epsilon_T + \epsilon_F$.

$\delta(E)$ for X-e scattering as follows [87,88]:

$$\omega_R = -\int_0^{\epsilon_F} dE \frac{\delta(E)}{\pi},$$
$$\omega_A = -\epsilon_T - \epsilon_F - \int_0^{\epsilon_F} dE \frac{\delta(E)}{\pi}. \quad (25)$$

The corresponding results are also shown in Figs. 6(a) and 7. The position of the attractive branch is well captured by the infinite mass model, while the shift of the repulsive one is underestimated. The doping dependence of the splitting between peaks is also linear, $\Delta\bar{\omega} = \epsilon_T + \epsilon_F$, but with the factor 1 instead of 3/2. This is not surprising since the reduced exciton-electron mass equals the electron mass $m$ in the case of the infinitely heavy exciton.

The doping dependence of the peak width $\gamma_{A(R)}$ is presented in Fig. 6(b). In the limit of vanishing doping, $\epsilon_F \ll \epsilon_X$, the widths of both XP branches are equal to the bare broadening for excitons $\gamma_X$. At finite doping, the repulsive XP linearly broadens with $\epsilon_F$, while the width of the attractive XP remains unchanged. This behavior agrees with observations both in TMDC monolayers [14] and in semiconductor QWs [89,90], and it is produced by both models with only a small difference between them, even at moderate doping, $\epsilon_F \sim \epsilon_T$.

Figure 6(c) shows the doping dependence of the spectral weight, $Z_{A(R)}$. While the total weight is conserved, $Z_R + Z_A = 1$, the doping results in a flow from the repulsive XP branch to the attractive XP branch until the former disappears. Again, we see a very good agreement between the results of the charge-dipole potential and those from the contact exciton-electron interaction. At a qualitative level, the behavior of the weights agrees with the experiment [14], which reported the dependence of absorption on the gate voltage that electrically controls the charge-carrier concentration in a TMDC monolayer.

## VI. DISCUSSION

In this work, we have focused on the experimentally relevant scenario where the photoexcited electron is distinguishable from those of the Fermi sea. The corresponding band arrangement, presented in Fig. 1, implies the presence of valley splitting in order for one of the Fermi seas to be depleted. Since the two valleys are time-reversal partners, this splitting can be induced either by exchange coupling with a ferromagnetic substrate or by a magnetic field [61–64]. As shown in a previous work by some of us [31], the magnetic field only weakly influences the polaronic physics as long as $\hbar\omega_B \ll \epsilon_T$, with $\omega_B = eB/mc$ the Larmor frequency for electrons. For a TMDC monolayer with $\epsilon_T \approx 20$ meV, this condition corresponds to $B \ll 57$ T, which is why even a magnetic field $B \sim 20$ T can still be considered rather weak. The combined effect of a magnetic substrate EuS [57] and a magnetic field 23 T [58] can be estimated to be 7.5 meV, which is sufficient to probe solely intervalley polaronic correlations, free from Pauli blocking and exchange physics.

We have demonstrated that at $\epsilon_F \ll \epsilon_X$, the X-e interactions can be approximated by a local potential that depends only on the relative distance between the exciton and the electron, and that its dependence on the doping is very weak. As a result, the presence of a Fermi sea of excess charge carriers only weakly influences the interactions, and they can be effectively addressed from the perspective of the three-particle trion problem. The recent comprehensive analysis of the energy-dependent phase shifts in the X-e scattering problem has demonstrated [48] that their low-energy behavior is well captured by classical charge-dipole interactions, in agreement with our results and conclusions.

The developed microscopic theory for XPs does not rely on any particular model for the screening of the Coulomb interactions. We have chosen the 2D Coulomb potential only due to the significant simplifications it provides in numerical calculations. This should predict the excited states in the excitonic spectrum reasonably well, while the ground state is instead well described by the Keldysh potential [67–69] that properly treats the dielectric screening in layered structures [17,70] (including TMDC monolayers embedded in hBN or deposited on a dielectric substrate). However, the universal classical charge-dipole behavior of the calculated X-e interactions suggests a natural generalization of our results to other potentials, including the Keldysh one. For instance, the X-e interactions can be approximated by modified charge-dipole interactions (19), which depend only on the polarizability of the excitonic state $\alpha$ and on the length $a_0$, which together incorporate the details of the screening and band structure. The polarizability can either be obtained from first-principles calculations [48,91–94] of the quadratic Stark effect for the ground excitonic state or it can be extracted from optical absorption measurements in the presence of a direct-current electric field. The value of $a_0$ can then be used as a free parameter to fit the splitting between the XP branches which, at low doping, is equal to the trion binding energy.

The scenario where the photoexcited electron is indistinguishable from those of the Fermi sea has been addressed within three-particle physics that is valid in the low-doping regime, $\epsilon_F \ll \epsilon_T$ [20]. In this case, exchange physics limits correlations, and trions (intravalley ones in TMDCs or spin-singlet ones in semiconductor QWs) are only stable if there is a strong imbalance between the masses of electrons and holes or in the presence of a strong magnetic field [95–99]. While experiments confirm this prediction, the interplay of exchange and polaronic physics is still poorly understood. This question can be naturally addressed based on our proposed variational

ansatz for the XP state, given by Eq. (5), but this is outside the scope of the present work.

We have focused on the polaronic splitting for the ground excitonic state $|0,0\rangle$ and have considered its coupling to the excited states perturbatively. The splitting for the excited state $|1,0\rangle$ (the other two states $|1,\pm1\rangle$ are optically dark) that has been recently reported [100–102] is outside the scope of the current work, but the ability of our approach to address this physics appears promising.

Details of the X-e interactions are especially important if they reside in closely spaced layers. The strong interlayer polaronic coupling opens new avenues to control the motion of excitons via the strong Coulomb drag effect [54], which cannot be captured by standard perturbative approaches [103]. Moreover, control over the flow of neutral excitons via electric and magnetic fields has recently been experimentally demonstrated [53].

To conclude, we have microscopically derived X-e interactions with the help of variational and perturbative approaches. The interactions only weakly depend on doping and can be well approximated by the classical charge-dipole potential. We have calculated the doping dependence of the optical conductivity and demonstrated that this is well captured by a model that instead uses a phenomenological exciton-electron contact potential. This indicates that including the finite range of interactions is not essential to capturing the physics of exciton polarons.

*Note added.* Recently, we became aware of a recent series of related papers [104–106]. These papers address the trion/exciton-polaron physics with coupled two- and four-particle correlation functions, and they are both consistent with and complementary to our microscopic theory based on the variational approach.

## ACKNOWLEDGMENTS

We acknowledge useful discussions with Francesca Maria Marchetti, Jonathan Keeling, and David Reichman. We acknowledge support from the Australian Research Council Centre of Excellence in Future Low-Energy Electronics Technologies (Grant No. CE170100039). J.L. is also supported through the Australian Research Council Future Fellowship No. FT160100244.

## APPENDIX A: PERTURBATION THEORY

This Appendix works through the perturbative approach to dealing with the contributions of excited states, $\phi_\nu$ and $\chi_{\nu\mathbf{k}\mathbf{k}'}$, in the variational equations (12). If we neglect interactions between the excited states themselves (since they are of second order in $\epsilon_T/\epsilon_X$), then these amplitudes become

$$\phi_\nu = \frac{\sum_{\mathbf{k}\mathbf{k}'} \Lambda^{\nu 0}_{\mathbf{k}-\mathbf{k}'} \chi_{0\mathbf{k}\mathbf{k}'}}{E^{\mathrm{XP}} - E^{\mathrm{X}}_\nu}, \tag{A1a}$$

$$\chi_{\nu\mathbf{k}\mathbf{k}'} = \frac{\Lambda^{\nu 0}_{\mathbf{k}'-\mathbf{k}}\phi_0 + \sum_{\bar{\mathbf{k}}} \Lambda^{\nu 0}_{\bar{\mathbf{k}}-\mathbf{k}} \chi_{0\bar{\mathbf{k}}\mathbf{k}'}}{E^{\mathrm{XP}} - E^{\mathrm{X}}_\nu - \epsilon^{\mathrm{FS}}_{\mathbf{k}\mathbf{k}'}}. \tag{A1b}$$

Note that in this section, momenta satisfy the conditions $k, \bar{k} > k_F$ and $k', \bar{k}' < k_F$ due to the presence of the Fermi sea. After inserting the above amplitudes into the equations for $\phi_0 \equiv \phi$ and $\chi_{0\mathbf{k}\mathbf{k}'} \equiv \chi_{\mathbf{k}\mathbf{k}'}$, which correspond to the ground state $|\nu\rangle = |0,0\rangle$, we obtain

$$\left(\Delta E^{\mathrm{XP}}_0 - \sum_{\mathbf{k}'} V_{\mathbf{k}'\mathbf{k}'\mathbf{k}'}\right)\phi = \sum_{\mathbf{k}\mathbf{k}'} V_{\mathbf{k}\mathbf{k}'\mathbf{k}'}\chi_{\mathbf{k}\mathbf{k}'}, \tag{A2a}$$

$$\left(\Delta E^{\mathrm{XP}}_0 - \epsilon^{\mathrm{FS}}_{\mathbf{k}\mathbf{k}'}\right)\chi_{\mathbf{k}\mathbf{k}'} = S_{\mathbf{k}\mathbf{k}'} + V_{\mathbf{k}'\mathbf{k}\mathbf{k}'}\phi + \sum_{\bar{\mathbf{k}}} V_{\bar{\mathbf{k}}\mathbf{k}\mathbf{k}'}\chi_{\bar{\mathbf{k}}\mathbf{k}'}. \tag{A2b}$$

Here, $\Delta E^{\mathrm{XP}}_0 = E^{\mathrm{XP}} - E^{\mathrm{X}}_0$ is the energy of the exciton-polaron state $E^{\mathrm{XP}}$ defined with respect to the energy of the excitonic ground state $E^{\mathrm{X}}_0$. These expressions (A2) coincide with the system of equations (16) presented in the main text, except for the additional term

$$S_{\mathbf{k}\mathbf{k}'} = \sum_{\nu\neq 0} \frac{\Lambda^{0\nu}_{\mathbf{k}'-\mathbf{k}}}{E^{\mathrm{XP}} - E^{\mathrm{X}}_\nu} \sum_{\bar{\mathbf{k}}\bar{\mathbf{k}}'} \Lambda^{\nu 0}_{\bar{\mathbf{k}}-\bar{\mathbf{k}}'}\chi_{\bar{\mathbf{k}}\bar{\mathbf{k}}'}. \tag{A3}$$

However, we now prove that this term is zero. First we note that due to rotational symmetry, $\chi_{\bar{\mathbf{k}}\bar{\mathbf{k}}'}$ above depends only on the relative angle $\theta_{\bar{\mathbf{k}}\bar{\mathbf{k}}'}$ between momenta $\bar{\mathbf{k}}$ and $\bar{\mathbf{k}}'$. Furthermore, the matrix element $\Lambda^{\nu 0}_{\bar{\mathbf{k}}-\bar{\mathbf{k}}'}$ can be factorized as $\Lambda^{\nu 0}_{\bar{\mathbf{k}}-\bar{\mathbf{k}}'} = \Pi_l\, e^{-il\theta_{\bar{\mathbf{k}}'}} F(\bar{k}, \bar{k}', \theta_{\bar{\mathbf{k}}\bar{\mathbf{k}}'})$ [see Eq. (C2) later]. Here, $\Pi_l = \sin(\pi|l|/2)$ is the parity factor that is nonzero for only odd values of $l$, and $F(\bar{k}, \bar{k}', \theta_{\bar{\mathbf{k}}\bar{\mathbf{k}}'})$ depends *only* on the relative angle between momenta $\theta_{\bar{\mathbf{k}}\bar{\mathbf{k}}'}$. If we shift the angular integration in Eq. (A3) to $d\theta_{\bar{\mathbf{k}}} d\theta_{\bar{\mathbf{k}}'} \to d\theta_{\bar{\mathbf{k}}\bar{\mathbf{k}}'} d\theta_{\bar{\mathbf{k}}'}$ and integrate over $d\theta_{\bar{\mathbf{k}}'}$, then we find that only excited states with $l = 0$ can contribute. However, their contribution in fact vanishes due to the parity factor $\Pi_0 = 0$. As a result, the term $S_{\mathbf{k}\mathbf{k}'}$ is zero and Eq. (A2) reduces to Eq. (16) in the main body.

## APPENDIX B: THE SPECTRUM OF EXCITONIC STATES

In this Appendix, we briefly review the analytic solution to the 2D Coulomb problem [78–80]. The spectrum consists of a discrete component that corresponds to bound excitons, and also a continuum of unbound electron-hole pairs. The discrete excitonic spectrum is labeled by radial $n = 0, 1, 2, \ldots$ and orbital $l = -n, \ldots, n$ quantum numbers. These can be combined into a single index $|\nu\rangle = |n, l\rangle$, which is used in the main text of the paper. The corresponding binding energies $E^{\mathrm{X}}_\nu = -\varkappa^2_\nu \epsilon_{\mathrm{X}}$ do not depend on $l$ and therefore feature the *accidental degeneracy* known for Coulomb problems [80]. Here, $\varkappa_\nu = 1/(2n+1)$, and $\epsilon_{\mathrm{X}} = me^4/\hbar^2\kappa^2$ is the binding energy for the ground excitonic state. The associated real-space wave functions $C^{nl}_{\mathbf{r}} = R_{nl}(r)\Phi_l(\theta_{\mathbf{r}})$ can be written as a product of the angular part $\Phi_l(\theta_{\mathbf{r}}) = e^{il\theta_{\mathbf{r}}}/\sqrt{2\pi}$ and the radial part $R_{nl}(r)$, given by

$$R_{nl}(r) = \frac{2\varkappa_\nu N_{nl}}{a_{\mathrm{X}}} \rho^{|l|} L^{2|l|}_{n-|l|}(\rho) e^{-\rho/2}. \tag{B1}$$

Above, $\rho = 2\varkappa_\nu r/a_{\mathrm{X}}$, and $a_{\mathrm{X}} = \hbar^2\kappa/me^2$ is the average separation between electron and hole in the excitonic ground state. In addition, $L^a_n(x)$ are generalized Laguerre polynomials and $N_{nl}$ is the normalization coefficient, where

$$N^2_{nl} = \varkappa_\nu \frac{(n-|l|)!}{(n+|l|)!}. \tag{B2}$$

The continuous spectrum for unbound electron-hole pairs is labeled by the dimensionless absolute momentum $q$ and the orbital quantum number $l = -\infty, \ldots, \infty$. Again, these can be combined into a single index $|\nu\rangle = |q, l\rangle$, and the corresponding energies are $E_\nu^{\rm X} = q^2\epsilon_{\rm X}$. The wave functions $C_{\mathbf{r}}^{ql} = R_{ql}(r)\Phi_l(\theta_{\mathbf{r}})$ can again be presented as a product where now the radial part $R_{ql}(r)$ is given by

$$R_{ql}(r) = \frac{2qN_{ql}}{a_{\rm X}}\rho^{|l|}{}_1F_1\left(\frac{i}{2q} + |l| + \frac{1}{2}, 2|l| + 1, i\rho\right)e^{-i\rho/2}. \tag{B3}$$

Here, $\rho = 2qr/a_{\rm X}$, and ${}_1F_1(a, b, z)$ is the Kummer confluent hypergeometric function. The normalization coefficient $N_{ql}$ is written as

$$N_{ql} = \frac{S_{ql}}{(2|l|)!}\sqrt{\frac{\pi/q}{1 + e^{-\pi/q}}}, \tag{B4}$$

where $S_{ql}$ is given by $S_{q0} = 1$ for $l = 0$ and

$$S_{ql} = \prod_{s=1}^{|l|}\sqrt{\left(s - \frac{1}{2}\right)^2 + \frac{1}{4q^2}} \tag{B5}$$

otherwise. The wave functions for bound excitonic states and unbound electron-hole pairs determine the X-e interactions via the matrix element for X-e scattering. This matrix element $\Lambda^{\nu\bar\nu}_{\mathbf{k}-\bar{\mathbf{k}}}$ is presented below in Appendix C.

## APPENDIX C: SCATTERING MATRIX ELEMENT

This Appendix discusses the matrix element $\Lambda^{\nu\bar\nu}_{\mathbf{k}-\bar{\mathbf{k}}}$ of X-e scattering with transferred momentum, $\mathbf{k} - \bar{\mathbf{k}}$. The exact expression for the scattering matrix element is

$$\Lambda^{\nu\bar\nu}_{\mathbf{k}-\bar{\mathbf{k}}} = U_{\mathbf{k}-\bar{\mathbf{k}}}\int d\mathbf{r}\left(C_{\mathbf{r}}^{\nu}\right)^* C_{\mathbf{r}}^{\bar\nu}\, 2i\sin\left[\frac{(\mathbf{k} - \bar{\mathbf{k}})\cdot\mathbf{r}}{2}\right]. \tag{C1}$$

By employing the explicit form of the spectrum from the 2D Coulomb problem, presented in Appendix B, this matrix element can be rewritten as follows:

$$\Lambda^{\nu\bar\nu}_{\mathbf{k}-\bar{\mathbf{k}}} = i\frac{2\pi e^2}{\kappa}\Pi_{l-\bar l}e^{i(\bar l - l)\theta_{\bar{\mathbf{k}}}}A^{\bar l - l}(k, \bar k, \theta_{\mathbf{k}\bar{\mathbf{k}}})M^{\nu\bar\nu}_{|\mathbf{k}-\bar{\mathbf{k}}|}, \tag{C2}$$

where $\theta_{\mathbf{k}\bar{\mathbf{k}}}$ is the relative angle between $\mathbf{k}$ and $\bar{\mathbf{k}}$. Here, the parity factor $\Pi_l$, the angle factor $A(k, \bar k, \theta_{\mathbf{k}\bar{\mathbf{k}}})$, and the integral $M_q^{\nu\bar\nu}$ are given by

$$\Pi_l = \sin\left(\frac{\pi|l|}{2}\right), \quad A(k, \bar k, \theta_{\mathbf{k}\bar{\mathbf{k}}}) = \frac{ke^{i\theta_{\mathbf{k}\bar{\mathbf{k}}}} - \bar k}{|\mathbf{k} - \bar{\mathbf{k}}|},$$
$$M_q^{\nu\bar\nu} = \int_0^\infty rdrR_\nu(r)R_{\bar\nu}(r)\frac{2}{q}J_{|l-\bar l|}\left(\frac{qr}{2}\right). \tag{C3}$$

Above, $R_\nu(r)$ is the radial part of the wave function $C_{\mathbf{r}}^{\nu}$, and $J_n(z)$ is the $n$th-order Bessel function of the first kind. Importantly, $\Pi_{l-\bar l}$ is nonzero only if $l - \bar l$ is odd, which implies that the states $|\nu\rangle$ and $|\bar\nu\rangle$ have opposite parities. For this reason, the matrix element of elastic X-e scattering is zero, $\Lambda^{\nu\nu}_{\mathbf{k}-\bar{\mathbf{k}}} = 0$, and hence X-e interactions appear only at second order in perturbation theory. (We discuss that further in Appendix E.) This argument is based solely on the symmetries of the excitonic states and is insensitive to details of the electron-hole interaction, $U_{\mathbf{q}}$. The latter impacts only on the magnitude of $M_q^{\nu\bar\nu}$.

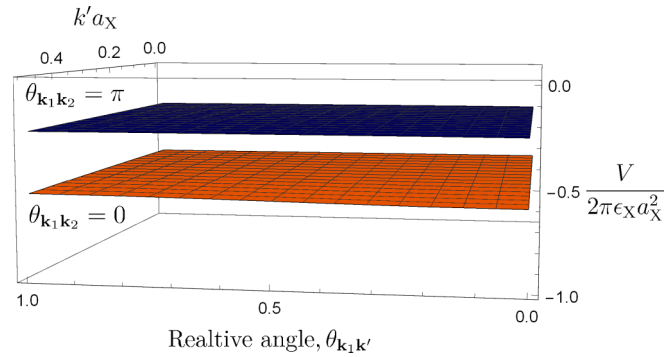


FIG. 8. Dependence of the nonlocal interaction, $V_{\mathbf{k}_1\mathbf{k}_2\mathbf{k}'}$, on both the magnitude $k'a_{\rm X}$ of the Fermi-hole momentum and its relative angle $\theta_{\mathbf{k}_1\mathbf{k}'}$. It is calculated for the momenta magnitudes $k_1a_{\rm X} = k_2a_{\rm X} = 1$ and for two values of the relative angle between them, $\theta_{\mathbf{k}_1\mathbf{k}_2} = 0$ and $\pi$.

## APPENDIX D: NONLOCAL EXCITON-ELECTRON INTERACTIONS

This Appendix presents a comparison between the microscopically derived nonlocal exciton-electron interaction $V_{\mathbf{k}_1\mathbf{k}_2\mathbf{k}'}$ (17) and its local approximation $V_{\rm L}(\mathbf{q})$ (18) with $\mathbf{q} = \mathbf{k}_1 - \mathbf{k}_2$. The nonlocal interaction potential $V_{\mathbf{k}_1\mathbf{k}_2\mathbf{k}'}$ is doping dependent and a function of three momenta $k_1$, $k_2$, $k'$ and two relative angles $\theta_{\mathbf{k}_1\mathbf{k}_2}$, $\theta_{\mathbf{k}_1\mathbf{k}'}$.

First, we notice that the dependence of the interaction $V_{\mathbf{k}_1\mathbf{k}_2\mathbf{k}'}$ on the momentum of the redundant Fermi hole, $k'$ and $\theta_{\mathbf{k}_1\mathbf{k}'}$, is extraordinarily weak for any $k_1$ and $k_2$ and $\theta_{\mathbf{k}_1\mathbf{k}_2}$. (Recall that this hole is not directly involved in the scattering event.) We illustrate this in Fig. 8 for $k_1a_{\rm X} = k_2a_{\rm X} = 1$ and for two values of their relative angle, $\theta_{\mathbf{k}_1\mathbf{k}_2} = 0$ and $\pi$. As a result, the nonlocal potential is very well approximated by its value at $\mathbf{k}' = \mathbf{0}$.

A preliminary comparison between the interactions, $V_{\mathbf{k}_1\mathbf{k}_20}$ and $V_{\rm L}(\mathbf{q})$, shows that the discrepancy between them, $\Delta V_{\mathbf{k}_1\mathbf{k}_2} = |V_{\mathbf{k}_1\mathbf{k}_20} - V_{\rm L}(\mathbf{q})|$, achieves a maximum at $k_1a_{\rm X} = k_2a_{\rm X}$. Their dependencies on these magnitudes of momenta and the angle between them, $\theta_{\mathbf{k}_1\mathbf{k}_2}$, are presented in Figs. 9 and 10 for $\epsilon_{\rm F}/\epsilon_{\rm X} = 0$ and 0.12 (respectively). Due to the ordering of energy scales, $\epsilon_{\rm T} \ll \epsilon_{\rm X}$, the length scale of the polaronic correlations is estimated to be $a_{\rm T} \approx a_{\rm X}\sqrt{\epsilon_{\rm X}/\epsilon_{\rm T}} \approx 3a_{\rm X}$, which corresponds to $qa_{\rm X} \sim 1/3$. It is clear that the local potential quite well approximates X-e interactions in the regime where $qa_{\rm X} \lesssim 1$. Therefore, the nonlocal nature of these interactions is important only at $qa_{\rm X} \gtrsim 1$, corresponding to an X-e separation that is smaller than the exciton size.

## APPENDIX E: EXCITON-ELECTRON SCATTERING

In this Appendix, we connect the matrix element $\Lambda^{\nu\bar\nu}_{\mathbf{q}}$ presented in Appendix C with the amplitude for X-e scattering. We additionally argue that the potential derived in Ref. [45] appears to be incorrect. If we treat the exciton as a structureless bosonic particle, then its scattering is solely determined

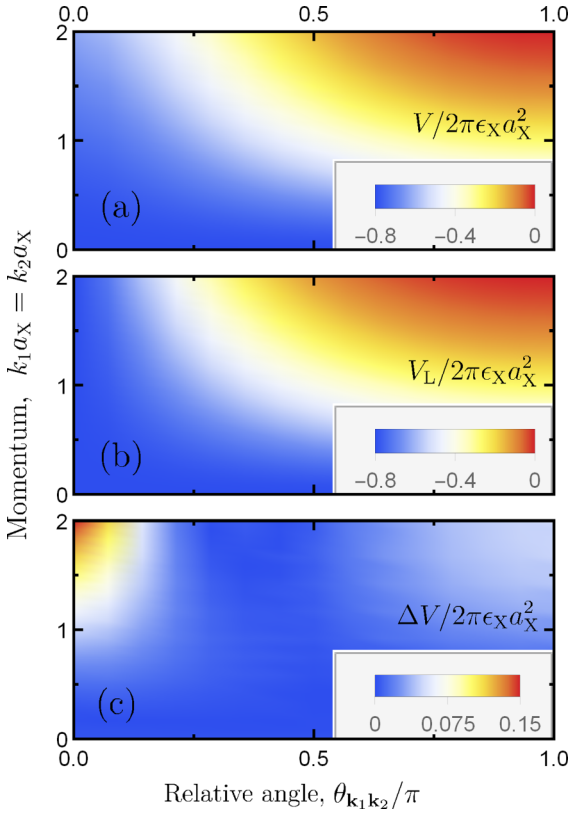


FIG. 9. (a) Nonlocal interactions $V_{\mathbf{k}_1\mathbf{k}_2\mathbf{0}}$, (b) the local one $V_L(\mathbf{q})$ with $\mathbf{q} = \mathbf{k}_1 - \mathbf{k}_2$, and (c) the discrepancy between them $\Delta V_{\mathbf{k}_1\mathbf{k}_2} = |V_{\mathbf{k}_1\mathbf{k}_2\mathbf{0}} - V_L(\mathbf{q})|$. Their dependencies on the momenta magnitudes $k_1 a_X = k_2 a_X$ and the relative angle $\theta_{\mathbf{k}_1\mathbf{k}_2}/\pi$ are depicted for $\epsilon_F = 0$.

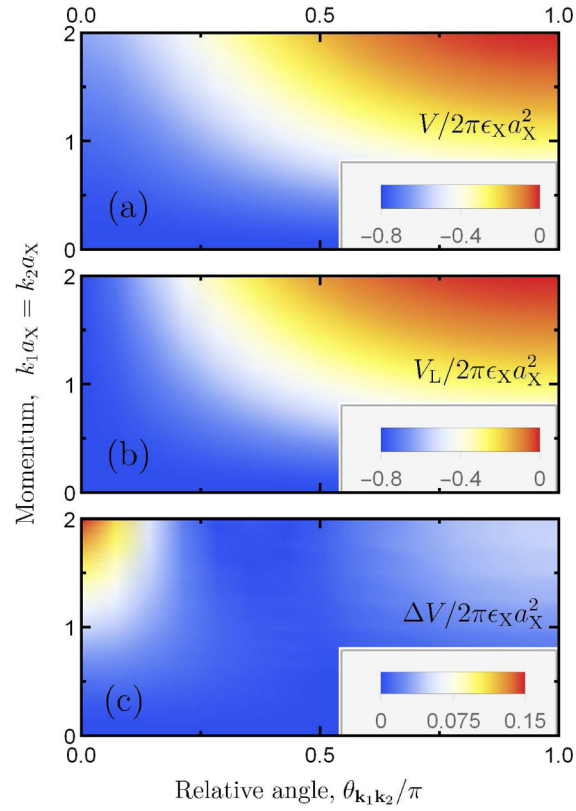


FIG. 10. (a) Nonlocal interactions $V_{\mathbf{k}_1\mathbf{k}_2\mathbf{0}}$, (b) the local one $V_L(\mathbf{q})$ with $\mathbf{q} = \mathbf{k}_1 - \mathbf{k}_2$, and (c) the discrepancy between them $\Delta V_{\mathbf{k}_1\mathbf{k}_2} = |V_{\mathbf{k}_1\mathbf{k}_2\mathbf{0}} - V_L(\mathbf{q})|$. Their dependencies on the momenta magnitudes $k_1 a_X = k_2 a_X$ and the relative angle $\theta_{\mathbf{k}_1\mathbf{k}_2}/\pi$ are depicted for $\epsilon_F = 0.12\,\epsilon_X$.

via interactions with electrons, $V_S(\mathbf{q})$. This can be expressed by the scattering amplitude within the Born approximation,

$$V_S(\mathbf{q}) = \langle f_0 | H_{X\text{-}e} | i_0 \rangle. \tag{E1}$$

Here, $|i_\nu\rangle = X^\dagger_{\nu\mathbf{p}_X} f^\dagger_{\mathbf{p}_e} |g\rangle$ and $|f_\nu\rangle = X^\dagger_{\nu\mathbf{p}_X+\mathbf{q}} f^\dagger_{\mathbf{p}_e-\mathbf{q}} |g\rangle$ are the excitonic states before and after scattering, with label $\nu$, and $|g\rangle$ is the unexcited Fermi sea. The electron $f^\dagger_{\mathbf{p}_e}$ and exciton $X^\dagger_{\nu\mathbf{p}_X}$ operators have been, respectively, introduced in Eqs. (1) and (4). Importantly, here, the exciton is assumed to reside in the ground state, $\nu = 0$, which indicates that the scattering is elastic.

The scattering matrix element (E1) can be evaluated microscopically by recalling the composite nature of the exciton and substituting $H_{X\text{-}e}$ with $H_{e\text{-}f} + H_{h\text{-}f}$ [the first and second terms in Eq. (2)]. A straightforward calculation $V_S(\mathbf{q}) = \Lambda^{00}_{\mathbf{q}}$ then yields

$$\begin{aligned} V_S(\mathbf{q}) &= \langle f_0 | (H_{e\text{-}f} + H_{h\text{-}f}) | i_0 \rangle \\ &= U_{\mathbf{q}} \sum_{\mathbf{p}} \left(C^0_{\mathbf{p}}\right)^* \left(C^0_{\mathbf{p}-\mathbf{q}/2} - C^0_{\mathbf{p}+\mathbf{q}/2}\right) = 0. \end{aligned} \tag{E2}$$

Above, $\Lambda^{\nu\bar{\nu}}_{\mathbf{q}}$ is the scattering matrix element between states $\nu$ and $\bar{\nu}$, which is discussed in Appendix C. We see that $V_S(\mathbf{q}) = 0$ because $\Lambda^{\nu\bar{\nu}}_{\mathbf{q}}$ is nonzero only between states of different parities (explained in Appendix C). Thus, we conclude that there is no contribution to X-e interactions from first-order perturbation theory. The vanishing scattering amplitude $V_S(\mathbf{q})$ reflects the fact that X-e interactions appear due to the polarization of the exciton by the electric field of the electron. This process appears at second order in perturbation theory, with no contribution at first order.


[1] K. S. Novoselov, A. K. Geim, S. V. Morozov, D. Jiang, Y. Zhang, S. V. Dubonos, I. V. Grigorieva, and A. A. Firsov, Electric field effect in atomically thin carbon films, Science **306**, 666 (2004).

[2] K. S. Novoselov, A. K. Geim, S. V. Morozov, D. Jiang, M. I. Katsnelson, I. V. Grigorieva, S. V. Dubonos, and A. A. Firsov, Two-dimensional gas of massless Dirac fermions in graphene, Nature (London) **438**, 197 (2005).

[3] A. K. Geim and A. H. MacDonald, Graphene: Exploring carbon flatland, Phys. Today **60**(8), 35 (2007).

[4] Y. Liu, Y. Gao, S. Zhang, J. He, J. Yu, and Z. Liu, Valleytronics in transition metal dichalcogenides materials, Nano Res. **12**, 2695 (2019).

[5] J. R. Schaibley, H. Yu, G. Clark, P. Rivera, J. S. Ross, K. L. Seyler, W. Yao, and X. Xu, Valleytronics in 2D materials, Nat. Rev. Mater. **1**, 16055 (2016).

[6] F. Xia, H. Wang, D. Xiao, M. Dubey, and A. Ramasubramaniam, Two-dimensional material nanophotonics, Nat. Photon. **8**, 899 (2014).

[7] H. Wang, L. Yu, Y.-H. Lee, Y. Shi, A. Hsu, M. L. Chin, L.-J. Li, M. Dubey, J. Kong, and T. Palacios, Integrated circuits based on bilayer $MoS_2$ transistors, Nano Lett. **12**, 4674 (2012).

[8] O. Lopez-Sanchez, D. Lembke, M. Kayci, A. Radenovic, and A. Kis, Ultrasensitive photodetectors based on monolayer $MoS_2$, Nat. Nanotechnol. **8**, 497 (2013).

[9] F. K. Perkins, A. L. Friedman, E. Cobas, P. M. Campbell, G. G. Jernigan, and B. T. Jonker, Chemical vapor sensing with monolayer $MoS_2$, Nano Lett. **13**, 668 (2013).

[10] J. Feng, X. Qian, C.-W. Huang, and J. Li, Strain-engineered artificial atom as a broad-spectrum solar energy funnel, Nat. Photon. **6**, 866 (2012).

[11] G. Wang, A. Chernikov, M. M. Glazov, T. F. Heinz, X. Marie, T. Amand, and B. Urbaszek, Colloquium: Excitons in atomically thin transition metal dichalcogenides, Rev. Mod. Phys. **90**, 021001 (2018).

[12] T. C. Berkelbach and D. R. Reichman, Optical and excitonic properties of atomically thin transition-metal dichalcogenides, Annu. Rev. Condens. Matter Phys. **9**, 379 (2018).

[13] M. V. Durnev and M. M. Glazov, Excitons and trions in two-dimensional semiconductors based on transition metal dichalcogenides, Phys. Usp. **61**, 825 (2018).

[14] A. Chernikov, A. M. van der Zande, H. M. Hill, A. F. Rigosi, A. Velauthapillai, J. Hone, and T. F. Heinz, Electrical Tuning of Exciton Binding Energies in Monolayer $WS_2$, Phys. Rev. Lett. **115**, 126802 (2015).

[15] F. Cadiz, S. Tricard, M. Gay, D. Lagarde, G. Wang, C. Robert, P. Renucci, B. Urbaszek, and X. Marie, Well separated trion and neutral excitons on superacid treated $MoS_2$ monolayers, Appl. Phys. Lett. **108**, 251106 (2016).

[16] B. Zhu, X. Chen, and X. Cui, Exciton binding energy of monolayer $WS_2$, Sci. Rep. **5**, 9218 (2015).

[17] C. Zhang, H. Wang, W. Chan, C. Manolatou, and F. Rana, Absorption of light by excitons and trions in monolayers of metal dichalcogenide $MoS_2$: Experiments and theory, Phys. Rev. B **89**, 205436 (2014).

[18] J. S. Ross, S. Wu, H. Yu, N. J. Ghimire, A. M. Jones, G. Aivazian, J. Yan, D. G. Mandrus, D. Xiao, W. Yao, and X. Xu, Electrical control of neutral and charged excitons in a monolayer semiconductor, Nat. Commun. **4**, 1474 (2013).

[19] K. F. Mak, K. He, C. Lee, G. H. Lee, J. Hone, T. F. Heinz, and J. Shan, Tightly bound trions in monolayer $MoS_2$, Nat. Mater. **12**, 207 (2013).

[20] E. Courtade, M. Semina, M. Manca, M. M. Glazov, C. Robert, F. Cadiz, G. Wang, T. Taniguchi, K. Watanabe, M. Pierre, W. Escoffier, E. L. Ivchenko, P. Renucci, X. Marie, T. Amand, and B. Urbaszek, Charged excitons in monolayer $WSe_2$: Experiment and theory, Phys. Rev. B **96**, 085302 (2017).

[21] One should note that photoluminescence experiments with ultraclean TMDC samples have also reported the presence of additional peaks, which have been attributed to biexcitons, localized excitons, and trions, as well as to four- and five-particle electron-hole complexes (e.g., [107,108]).

[22] It should be noted that this phenomenon has been observed in conventional semiconductor GaAs and CdTe quantum wells (QWs) [89,90,109–111]. However, the binding energies $\epsilon_X$ and $\epsilon_T$ in QWs are more than an order of magnitude smaller than in TMDC monolayers, and this restricts the observability of phenomena in QWs to very low temperatures.

[23] D. W. Kidd, D. K. Zhang, and K. Varga, Binding energies and structures of two-dimensional excitonic complexes in transition metal dichalcogenides, Phys. Rev. B **93**, 125423 (2016).

[24] B. Ganchev, N. Drummond, I. Aleiner, and V. Fal'ko, Three-Particle Complexes in Two-Dimensional Semiconductors, Phys. Rev. Lett. **114**, 107401 (2015).

[25] K. A. Velizhanin and A. Saxena, Excitonic effects in two-dimensional semiconductors: Path integral Monte Carlo approach, Phys. Rev. B **92**, 195305 (2015).

[26] M. Z. Mayers, T. C. Berkelbach, M. S. Hybertsen, and D. R. Reichman, Binding energies and spatial structures of small carrier complexes in monolayer transition-metal dichalcogenides via diffusion Monte Carlo, Phys. Rev. B **92**, 161404(R) (2015).

[27] Y. V. Zhumagulov, A. Vagov, N. Y. Senkevich, D. R. Gulevich, and V. Perebeinos, Three-particle states and brightening of intervalley excitons in a doped $MoS_2$ monolayer, Phys. Rev. B **101**, 245433 (2020).

[28] Y. V. Zhumagulov, A. Vagov, D. R. Gulevich, P. E. F. Junior, and V. Perebeinos, Trion induced photoluminescence of a doped $MoS_2$ monolayer, J. Chem. Phys. **153**, 044132 (2020).

[29] M. Sidler, P. Back, O. Cotlet, A. Srivastava, T. Fink, M. Kroner, E. Demler, and A. Imamoglu, Fermi polaron-polaritons in charge-tunable atomically thin semiconductors, Nat. Phys. **13**, 255 (2016).

[30] D. K. Efimkin and A. H. MacDonald, Many-body theory of trion absorption features in two-dimensional semiconductors, Phys. Rev. B **95**, 035417 (2017).

[31] D. K. Efimkin and A. H. MacDonald, Exciton-polarons in doped semiconductors in a strong magnetic field, Phys. Rev. B **97**, 235432 (2018).

[32] R. Suris, V. Kochereshko, G. Astakhov, D. Yakovlev, W. Ossau, J. Nurnberger, W. Faschinger, G. Landwehr, T. Wojtowicz, G. Karczewski, and J. Kossut, Excitons and trions modified by interaction with a two-dimensional electron gas, Phys. Status Solidi B **227**, 343 (2001).

[33] R. Suris, in *Optical Properties of 2D Systems with Interacting Electrons*, edited by W. Ossau and R. A. Suris (NATO Scientific Series, Kluwe, 2000).

[34] M. Baeten and M. Wouters, Polariton formation in a microcavity with a doped quantum well: Roles of the Fermi edge singularity and Anderson orthogonality catastrophe, Phys. Rev. B **89**, 245301 (2014).

[35] M. Baeten and M. Wouters, Many-body effects of a two-dimensional electron gas on trion-polaritons, Phys. Rev. B **91**, 115313 (2015).

[36] M. Combescot, J. Tribollet, G. Karczewski, F. Bernardot, C. Testelin, and M. Chamarro, Many-body origin of the "trion line" in doped quantum wells, Europhys. Lett. **71**, 431 (2005).

[37] S.-Y. Shiau, M. Combescot, and Y.-C. Chang, Trion ground state, excited states, and absorption spectrum using electron-exciton basis, Phys. Rev. B **86**, 115210 (2012).

[38] M. Combescot, O. Betbeder-Matibet, and F. Dubin, The trion: Two electrons plus one hole versus one electron plus one exciton, Eur. Phys. J. B **42**, 63 (2004).

[39] A. Esser, R. Zimmermann, and E. Runge, Theory of trion spectra in semiconductor nanostructures, Phys. Status Solidi B **227**, 317 (2001).

[40] P. Massignan, M. Zaccanti, and G. M. Bruun, Polarons, dressed molecules and itinerant ferromagnetism in ultracold Fermi gases, Rep. Prog. Phys. **77**, 034401 (2014).

[41] J. Levinsen and M. M. Parish, Chapter 1: Strongly interacting two-dimensional Fermi gases, Annu. Rev. Cold Atoms Mol. **3**, 1 (2015).

[42] D. Van Tuan, B. Scharf, Z. Wang, J. Shan, K. F. Mak, I. Žutić, and H. Dery, Probing many-body interactions in monolayer transition-metal dichalcogenides, Phys. Rev. B **99**, 085301 (2019).

[43] D. Van Tuan, B. Scharf, I. Žutić, and H. Dery, Marrying Excitons and Plasmons in Monolayer Transition-Metal Dichalcogenides, Phys. Rev. X **7**, 041040 (2017).

[44] B. Scharf, D. V. Tuan, I. Žutić, and H. Dery, Dynamical screening in monolayer transition-metal dichalcogenides and its manifestations in the exciton spectrum, J. Condens. Matter Phys. **31**, 203001 (2019).

[45] Y.-W. Chang and D. R. Reichman, Many-body theory of optical absorption in doped two-dimensional semiconductors, Phys. Rev. B **99**, 125421 (2019).

[46] Y.-C. Chang, S.-Y. Shiau, and M. Combescot, Crossover from trion-hole complex to exciton-polaron in *n*-doped two-dimensional semiconductor quantum wells, Phys. Rev. B **98**, 235203 (2018).

[47] M. M. Glazov, Optical properties of charged excitons in two-dimensional semiconductors, J. Chem. Phys. **153**, 034703 (2020).

[48] C. Fey, P. Schmelcher, A. Imamoglu, and R. Schmidt, Theory of exciton-electron scattering in atomically thin semiconductors, Phys. Rev. B **101**, 195417 (2020).

[49] L. B. Tan, O. Cotlet, A. Bergschneider, R. Schmidt, P. Back, Y. Shimazaki, M. Kroner, and A. İmamoğlu, Interacting Polaron-Polaritons, Phys. Rev. X **10**, 021011 (2020).

[50] O. Kyriienko, D. N. Krizhanovskii, and I. A. Shelykh, Nonlinear Quantum Optics with Trion-Polaritons in 2D Monolayers: Conventional and Unconventional Photon Blockade, Phys. Rev. Lett. **125**, 197402 (2020).

[51] R. P. A. Emmanuele, M. Sich, O. Kyriienko, V. Shahnazaryan, F. Withers, A. Catanzaro, P. M. Walker, F. A. Benimetskiy, M. S. Skolnick, A. I. Tartakovskii, I. A. Shelykh, and D. N. Krizhanovskii, Highly nonlinear trion-polaritons in a monolayer semiconductor, Nat. Commun. **11**, 3589 (2020).

[52] M. A. Bastarrachea-Magnani, A. Camacho-Guardian, and G. M. Bruun, Attractive and repulsive exciton-polariton interactions mediated by an electron gas, arXiv:2008.10303.

[53] T. Chervy, P. Knüppel, H. Abbaspour, M. Lupatini, S. Fält, W. Wegscheider, M. Kroner, and A. Imamoğlu, Accelerating Polaritons with External Electric and Magnetic Fields, Phys. Rev. X **10**, 011040 (2020).

[54] O. Cotleţ, F. Pientka, R. Schmidt, G. Zarand, E. Demler, and A. Imamoglu, Transport of Neutral Optical Excitations Using Electric Fields, Phys. Rev. X **9**, 041019 (2019).

[55] R. A. Sergeev and R. A. Suris, Ground-state energy of $X^-$ and $X^+$ trions in a two-dimensional quantum well at an arbitrary mass ratio, Phys. Solid State **43**, 746 (2001).

[56] A. Thilagam, Two-dimensional charged-exciton complexes, Phys. Rev. B **55**, 7804 (1997).

[57] C. Zhao, T. Norden, P. Zhang, P. Zhao, Y. Cheng, F. Sun, J. P. Parry, P. Taheri, J. Wang, Y. Yang, T. Scrace, K. Kang, S. Yang, G.-x. Miao, R. Sabirianov, G. Kioseoglou, W. Huang, A. Petrou, and H. Zeng, Enhanced valley splitting in monolayer $WSe_2$ due to magnetic exchange field, Nat. Nanotechnol. **12**, 757 (2017).

[58] T. Smoleński, O. Cotlet, A. Popert, P. Back, Y. Shimazaki, P. Knüppel, N. Dietler, T. Taniguchi, K. Watanabe, M. Kroner, and A. Imamoglu, Interaction-Induced Shubnikov–de Haas Oscillations in Optical Conductivity of Monolayer $MoSe_2$, Phys. Rev. Lett. **123**, 097403 (2019).

[59] M. M. Parish, F. M. Marchetti, and P. B. Littlewood, Supersolidity in electron-hole bilayers with a large density imbalance, Europhys. Lett. **95**, 27007 (2011).

[60] O. Cotlet, D. S. Wild, M. D. Lukin, and A. Imamoglu, Rotons in optical excitation spectra of monolayer semiconductors, Phys. Rev. B **101**, 205409 (2020).

[61] A. Srivastava, M. Sidler, A. V. Allain, D. S. Lembke, A. Kis, and A. Imamoglu, Valley Zeeman effect in elementary optical excitations of monolayer $WSe_2$, Nat. Phys. **11**, 141 (2015).

[62] G. Aivazian, Z. Gong, A. M. Jones, R.-l. Chu, J. Yan, D. G. Mandrus, C. Zhang, D. Cobden, W. Yao, and X. Xu, Magnetic control of valley pseudospin in monolayer $WSe_2$, Nat. Phys. **11**, 148 (2015).

[63] D. MacNeill, C. Heikes, K. F. Mak, Z. Anderson, A. Kormányos, V. Zólyomi, J. Park, and D. C. Ralph, Breaking of Valley Degeneracy by Magnetic Field in Monolayer $MoSe_2$, Phys. Rev. Lett. **114**, 037401 (2015).

[64] Z. Wang, J. Shan, and K. F. Mak, Valley- and spin-polarized Landau levels in monolayer $WSe_2$, Nat. Nanotechnol. **12**, 144 (2016).

[65] The polaronic effect leads to a splitting only when there is an electron-hole mass imbalance [20]. However, this imbalance is removed for TMDC monolayers and also in the presence of a magnetic field [112–114].

[66] The exciton-polaron state comprises only a single photoexcited electron-hole pair. As a result, both electron-electron and hole-hole interactions are irrelevant for absorption and might only be important for nonlinear optical effects that are outside the scope of this work.

[67] L. V. Keldysh, Coulomb interaction in thin semiconductor and semimetal films, JETP Lett. **29**, 658 (1979).

[68] N. S. Rytova, The screened potential of a point charge in a thin film, Moscow Univ. Phys. Bull. **3**, 18 (1967).

[69] P. Cudazzo, I. V. Tokatly, and A. Rubio, Dielectric screening in two-dimensional insulators: Implications for excitonic and impurity states in graphane, Phys. Rev. B **84**, 085406 (2011).

[70] A. Chernikov, T. C. Berkelbach, H. M. Hill, A. Rigosi, Y. Li, O. B. Aslan, D. R. Reichman, M. S. Hybertsen, and T. F. Heinz, Exciton Binding Energy and Nonhydrogenic Rydberg Series in Monolayer $WS_2$, Phys. Rev. Lett. **113**, 076802 (2014).

[71] M. Koschorreck, D. Pertot, E. Vogt, B. Fröhlich, M. Feld, and M. Köhl, Attractive and repulsive Fermi polarons in two dimensions, Nature (London) **485**, 619 (2012).

[72] Y. Zhang, W. Ong, I. Arakelyan, and J. E. Thomas, Polaron-to-Polaron Transitions in the Radio-Frequency Spectrum of a Quasi-Two-Dimensional Fermi Gas, Phys. Rev. Lett. **108**, 235302 (2012).

[73] N. Darkwah Oppong, L. Riegger, O. Bettermann, M. Höfer, J. Levinsen, M. M. Parish, I. Bloch, and S. Fölling, Observation of Coherent Multiorbital Polarons in a Two-Dimensional Fermi Gas, Phys. Rev. Lett. **122**, 193604 (2019).

[74] F. Chevy, Universal phase diagram of a strongly interacting Fermi gas with unbalanced spin populations, Phys. Rev. A **74**, 063628 (2006).

[75] R. Combescot and S. Giraud, Normal State of Highly Polarized Fermi Gases: Full Many-Body Treatment, Phys. Rev. Lett. **101**, 050404 (2008).

[76] S. Zöllner, G. M. Bruun, and C. J. Pethick, Polarons and molecules in a two-dimensional Fermi gas, Phys. Rev. A **83**, 021603(R) (2011).

[77] M. M. Parish and J. Levinsen, Highly polarized Fermi gases in two dimensions, Phys. Rev. A **87**, 033616 (2013).

[78] Calvin Yi-Ping Chao and S. L. Chuang, Analytical and numerical solutions for a two-dimensional exciton in momentum space, Phys. Rev. B **43**, 6530 (1991).

[79] X. L. Yang, S. H. Guo, F. T. Chan, K. W. Wong, and W. Y. Ching, Analytic solution of a two-dimensional hydrogen atom. I. Nonrelativistic theory, Phys. Rev. A **43**, 1186 (1991).

[80] D. G. W. Parfitt and M. E. Portnoi, The two-dimensional hydrogen atom revisited, J. Math. Phys. **43**, 4681 (2002).

[81] S. Glutch, *Excitons in Low-dimensional Semiconductors: Theory, Numerical Methods, Applications* (Springer, Berlin, 2004).

[82] G. Ramon, A. Mann, and E. Cohen, Theory of neutral and charged exciton scattering with electrons in semiconductor quantum wells, Phys. Rev. B **67**, 045323 (2003).

[83] M. R. Carbone, M. Z. Mayers, and D. R. Reichman, Microscopic model of the doping dependence of linewidths in monolayer transition metal dichalcogenides, J. Chem. Phys. **152**, 194705 (2020).

[84] In the balanced case $m_e = m_h$, the nonzero $V_S(\mathbf{q})$ was mistakenly claimed in Ref. [45], but resolved thereafter [83], D. Reichman (private communication).

[85] The optical conductivity is an even function of the frequency $\omega$ and, within linear response theory, can be presented as $\sigma_{\text{total}}(\omega) = \sigma(\omega) + \sigma(-\omega)$, with $\sigma(\omega)$ given by Eq. (22). In the frequency range $\omega \sim \epsilon_g$, the second term is negligible and can be safely omitted.

[86] M. M. Parish and J. Levinsen, Quantum dynamics of impurities coupled to a Fermi sea, Phys. Rev. B **94**, 184303 (2016).

[87] D. Pimenov and M. Goldstein, Spectra of heavy polarons and molecules coupled to a Fermi sea, Phys. Rev. B **98**, 220302(R) (2018).

[88] F. Fumi, CXVI. Vacancies in monovalent metals, London Edinburgh Dublin Philos. Mag. J. Sci. **46**, 1007 (1955).

[89] G. V. Astakhov, V. P. Kochereshko, D. R. Yakovlev, W. Ossau, J. Nürnberger, W. Faschinger, and G. Landwehr, Oscillator strength of trion states in ZnSe-based quantum wells, Phys. Rev. B **62**, 10345 (2000).

[90] V. Huard, R. T. Cox, K. Saminadayar, A. Arnoult, and S. Tatarenko, Bound States in Optical Absorption of Semiconductor Quantum Wells Containing a Two-Dimensional Electron Gas, Phys. Rev. Lett. **84**, 187 (2000).

[91] B. Scharf, T. Frank, M. Gmitra, J. Fabian, I. Žutić, and V. Perebeinos, Excitonic Stark effect in $MoS_2$ monolayers, Phys. Rev. B **94**, 245434 (2016).

[92] S. Haastrup, S. Latini, K. Bolotin, and K. S. Thygesen, Stark shift and electric-field-induced dissociation of excitons in monolayer $MoS_2$ and $h$BN/$MoS_2$ heterostructures, Phys. Rev. B **94**, 041401(R) (2016).

[93] T. G. Pedersen, Exciton Stark shift and electroabsorption in monolayer transition-metal dichalcogenides, Phys. Rev. B **94**, 125424 (2016).

[94] L. S. R. Cavalcante, D. R. da Costa, G. A. Farias, D. R. Reichman, and A. Chaves, Stark shift of excitons and trions in two-dimensional materials, Phys. Rev. B **98**, 245309 (2018).

[95] J. J. Palacios, D. Yoshioka, and A. H. MacDonald, Long-lived charged multiple-exciton complexes in strong magnetic fields, Phys. Rev. B **54**, R2296 (1996).

[96] A. B. Dzyubenko, Charged hydrogenic problem in a magnetic field: Noncommutative translations, unitary transformations, and coherent states, Phys. Rev. B **65**, 035318 (2001).

[97] A. B. Dzyubenko and A. Y. Sivachenko, Charged Magnetoexcitons in Two-Dimensions: Magnetic Translations and Families of Dark States, Phys. Rev. Lett. **84**, 4429 (2000).

[98] A. Wójs and J. J. Quinn, Exact-diagonalization studies of trion energy spectra in high magnetic fields, Phys. Rev. B **75**, 085318 (2007).

[99] A. Wójs, J. J. Quinn, and P. Hawrylak, Charged excitons in a dilute two-dimensional electron gas in a high magnetic field, Phys. Rev. B **62**, 4630 (2000).

[100] A. Arora, T. Deilmann, T. Reichenauer, J. Kern, S. Michaelis de Vasconcellos, M. Rohlfing, and R. Bratschitsch, Excited-State Trions in Monolayer $WS_2$, Phys. Rev. Lett. **123**, 167401 (2019).

[101] T. Goldstein, Y.-C. Wu1, S.-Y. Chen, T. Taniguchi, K. Watanabe, K. Varga, and J. Yan, Ground and excited state exciton polarons in monolayer $MoSe_2$, J. Chem. Phys. **153**, 071101 (2020).

[102] K. Wagner, E. Wietek, J. D. Ziegler, M. A. Semina, T. Taniguchi, K. Watanabe, J. Zipfel, M. M. Glazov, and A. Chernikov, Autoionization and Dressing of Excited Excitons by Free Carriers in Monolayer $WSe_2$, Phys. Rev. Lett. **125**, 267401 (2020).

[103] B. N. Narozhny and A. Levchenko, Coulomb drag, Rev. Mod. Phys. **88**, 025003 (2016).

[104] F. Rana, O. Koksal, M. Jung, G. Shvets, and C. Manolatou, Many-body theory of radiative lifetimes of exciton-trion superposition states in doped two-dimensional materials, Phys. Rev. B **103**, 035424 (2021).

[105] F. Rana, O. Koksal, and C. Manolatou, Many-body theory of the optical conductivity of excitons and trions in two-dimensional materials, Phys. Rev. B **102**, 085304 (2020).

[106] F. Rana, O. Koksal, M. Jung, G. Shvets, A. N. Vamivakas, and C. Manolatou, Exciton-trion-polaritons in two-dimensional materials, arXiv:2009.13069.

[107] S.-Y. Chen, T. Goldstein, T. Taniguchi, K. Watanabe, and J. Yan, Coulomb-bound four- and five-particle intervalley states in an atomically-thin semiconductor, Nat. Commun. **9**, 3717 (2018).

[108] Z. Li, T. Wang, Z. Lu, C. Jin, Y. Chen, Y. Meng, Z. Lian, T. Taniguchi, K. Watanabe, S. Zhang, D. Smirnov, and S.-F. Shi, Revealing the biexciton and trion-exciton complexes in BN encapsulated $WSe_2$, Nat. Commun. **9**, 3719 (2018).

[109] G. Yusa, H. Shtrikman, and I. Bar-Joseph, Onset of exciton absorption in modulation-doped GaAs quantum wells, Phys. Rev. B **62**, 15390 (2000).

[110] V. Ciulin, P. Kossacki, S. Haacke, J.-D. Ganière, B. Deveaud, A. Esser, M. Kutrowski, and T. Wojtowicz, Radiative behavior of negatively charged excitons in CdTe-based quantum wells: A spectral and temporal analysis, Phys. Rev. B **62**, R16310 (2000).

[111] K. Kheng, R. T. Cox, Merle Y. d' Aubigné, F. Bassani, K. Saminadayar, and S. Tatarenko, Observation of Negatively Charged Excitons $X^-$ in Semiconductor Quantum Wells, Phys. Rev. Lett. **71**, 1752 (1993).

[112] C. Schüller, K.-B. Broocks, C. Heyn, and D. Heitmann, Oscillator strengths of dark charged excitons at low electron filling factors, Phys. Rev. B **65**, 081301(R) (2002).

[113] D. Andronikov, V. Kochereshko, A. Platonov, T. Barrick, S. A. Crooker, and G. Karczewski, Singlet and triplet trion states in high magnetic fields: Photoluminescence and reflectivity spectra of modulation-doped $CdTeCd_{0.7}Mg_{0.3}Te$ quantum wells, Phys. Rev. B **72**, 165339 (2005).

[114] D. Sanvitto, D. M. Whittaker, A. J. Shields, M. Y. Simmons, D. A. Ritchie, and M. Pepper, Origin of the Oscillator Strength of the Triplet State of a Trion in a Magnetic Field, Phys. Rev. Lett. **89**, 246805 (2002).